The Pennsylvania State University

The Graduate School

Department of Mechanical and Nuclear Engineering

QUANTIFYING THE IMPACT OF FUNCTIONALLY GRADED MATERIALS ON THE FATIGUE LIFE OF MATERIAL JETTED SPECIMENS

A Thesis in

Mechanical Engineering

by

Dorcas V. Kaweesa

Submitted in Partial Fulfillment
of the Requirements
for the Degree of

Master of Science

December 2017

The thesis of Dorcas V. Kaweesa was reviewed and approved* by the following:

Nicholas A. Meisel
Assistant Professor, Engineering Design and Mechanical Engineering
Thesis Advisor

Timothy W. Simpson
Paul Morrow Professor of Engineering Design and Manufacturing

Karen Thole
Department Head and Distinguished Professor
Mechanical and Nuclear Engineering

*Signatures are on file in the Graduate School

ABSTRACT

The capability of Additive Manufacturing (AM) to process multiple materials allows the fabrication of complex and multifunctional parts with varying mechanical properties. Multi-material AM involves the fabrication of 3D printed objects with multiple heterogeneous material compositions. The material jetting AM process, specifically the PolyJet process, has the capacity and capability to manufacture multi-material structures with both rigid and flexible material properties. Existing research has investigated the fatigue properties of 3D printed multi-material specimens and shows that there is a weakness at the multi-material interface. This research seeks to investigate the effects of material gradient transitions on the fatigue life and failure predictability of 3D printed multi-material specimens given (1) a constant volume or (2) a constant length of a flexible material. In order to analyze the fatigue life at the material interface, discrete material gradients are compared against continuous material gradients created through voxel-level design. Furthermore, individual material composites are analyzed in relation to their material properties. Results demonstrate the effects of material gradient transitions on the fatigue life as well as the qualitative material properties of the continuous and discrete material gradients. In addition, results from studying individual material composites helps understand the effect of different material gradients on material properties of multi-material parts.

TABLE OF CONTENTS

LIST OF FIGURES

LIST OF TABLES

ACKNOWLEDGEMENTS

I would like to thank each and every one who has made it possible for me to achieve this degree. I specially would like to thank:

Dr. Nicholas Meisel, for accepting me into the Made By Design Lab and for continually guiding me to become a creative and independent researcher.

Dr. Timothy Simpson, for supporting my endeavors in learning more about additive manufacturing.

Dr. Manahan and the MP Machinery and Testing, for assisting in performing fatigue tests.

Dr. Hickner and Dr. Beese, for your assistance in the approval of access to the Material Testing Laboratory.

Phil Irwin in the Department of Mechanical and Nuclear Engineering Machine workshop, for kindly providing machining services so that my testing procedures could be successful.

Made By Design Lab members, for your friendship and support in providing valuable insights on various ideas.

Dr. Amy Freeman and Dr. Wayne Gersie from the Center for Engineering Outreach and Inclusion for providing support and a sense of community through the Multicultural Engineering Program.

Lastly, the Kaweesa family; Dad, Mum, Elizabeth, and Samuel, as well as Tabitha and Joseph Mwesige, for being my strongest support system while pursuing this degree and for believing in and always encouraging me to aim higher.

Chapter 1

INTRODUCTION AND MOTIVATION

1.1 Overview of Multi-Material AM

Additive Manufacturing (AM), commonly known as 3D printing, is a process that involves joining materials to make objects generated from 3D CAD model data [1]. The layer-by-layer deposition of materials enables the production of geometrically complex structures that cannot be manufactured by traditional means. Additionally, AM provides better structural optimization, offers low volume production, allows part consolidation, and maximizes design flexibility. These advantages provide opportunities for designing and manufacturing parts with heterogeneous material compositions. Due to the design freedom and material complexity afforded by AM technology, engineers and designers can design complex structures by incorporating different material profiles into digital models, which are then reproduced through compatible AM processes. For example, combining materials with rigid and flexible properties leads to structures with varying material properties that span throughout the volume of the structure [2].

Currently, the only AM processes that are capable of producing parts with multiple materials include material extrusion, directed energy deposition (DED), and material jetting. Figure 1-1 shows schematics of the material extrusion and the DED processes. Multi-materials are manufactured via material extrusion systems by simultaneously

extruding layers of material through two different nozzles. Even though material extrusion thermoplastics are known for their substantial resistance to high temperatures and strength, the print layers exhibit stair stepping edges, which cause stress concentrations that weaken the printed part [3,4]. The DED process, on the other hand, involves the deposition of material in powder or wire form and energy through a laser or an electron beam that is directed at the exact point of contact of material addition.

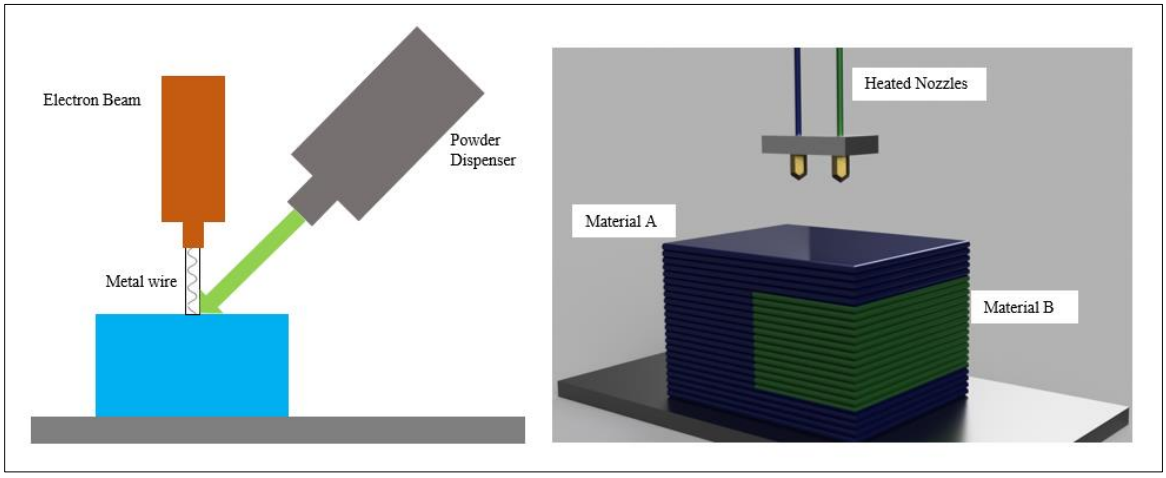

Figure **1-1**: Schematics of the material extrusion (left) and the DED (right) processes.

Within the scope of this research, the capabilities provided by the material jetting process were investigated. Figure 1-2 shows a schematic of the material jetting process. The material jetting process, according to the Standard Terminology for AM Technologies [5], is an AM process in which droplets of liquid-based photopolymer material are selectively deposited by jetting. During the process of photopolymer deposition, the liquid photopolymer is cured using ultraviolet (UV) light, incorporated in the print chamber, to initialize the polymerization reaction process. The resin solidifies as a result of curing and the process continues as additional layers are deposited. Subsequent

layers are deposited in the Z-direction, on top of the previously cured layer until a final part is obtained [6–8].

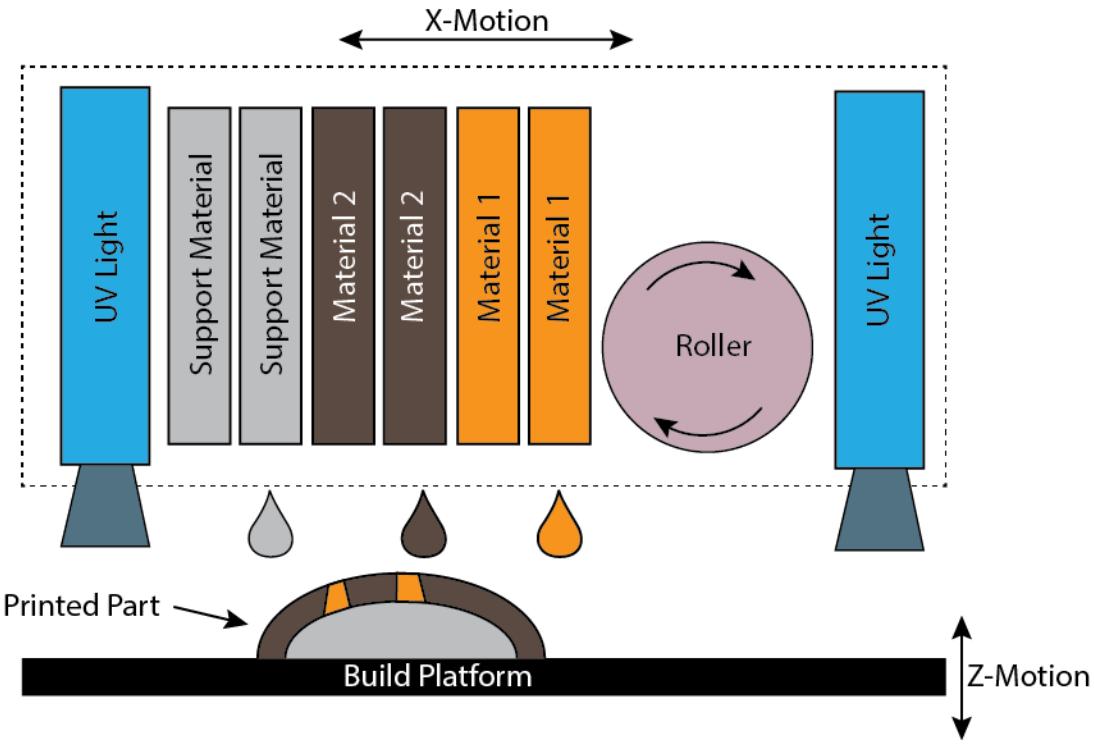

Figure **1-2**: Schematic showing the material jetting printing process.

An example of the material jetting process is the PolyJet™ process (Stratasys Ltd., MN), which involves the simultaneous jetting of two or more photopolymers in a drop-on-demand deposition manner. For example, the common materials TangoBlackPlus™ (TB+) (Stratasys Ltd., MN) and VeroWhitePlus™ (VW+) (Stratasys Ltd., MN), which have flexible and rigid materials properties respectively, are important in designing compliant structures. With the high end accuracy of the process' high resolution capabilities [9] along with a minimum layer thickness of 16 µm in the build layers and multiple printing modes, the process is capable of finely controlling the compositions of

such materials through voxel-based deposition using a dithering design approach. The dithering approach involves contrasting pixels of colors to create an impression of a third intermediate color. In addition, the PolyJet process uses an array of multiple ink-jet print heads to deposit different concentrations of material through gradual suspension within the matrix of a structure's volume. By controlling the material compositions at the voxel-level, functionally graded materials can be created with varying material composition profiles. These characteristics specifically distinguish the PolyJet process from the material extrusion and DED processes, which do not possess such capabilities.

The use of multi-materials within the PolyJet process has advantages in the area of functionally graded materials (FGMs). FGMs are heterogeneous materials consisting of two or more constituent materials that spatially vary in their material composition across the volume of a structure [10–12]. Using the material complexity and design freedom provided by AM, FGMs can be manipulated to control material properties such as strength, stiffness, toughness, and flexibility within a multi-material structure based on the material composition at the microstructural level. As illustrated in the Figure 1-3 below, Material A and Material B are varied across the volume of the structure from on end to the other to form a material gradient transition region [13].

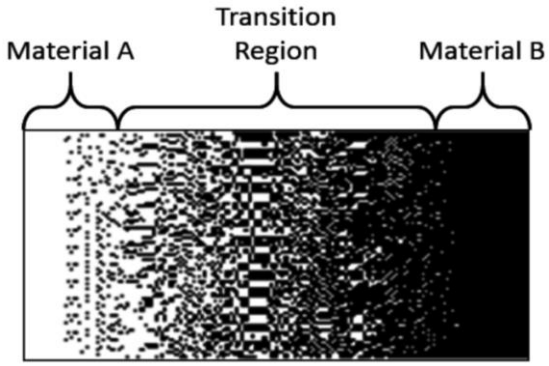

Figure **1-3**: Example of a functionally graded structure with a gradient transition between material A and material B.

The material concentration, shape, and orientation of constituent materials can be gradually changed in different directions to optimize FGMs behavior within a structure [13]. By applying appropriate concentrations of material, it is possible to develop functionally graded structures with improved material properties such as structural strength, stiffness, and fatigue behavior. FGMs are useful tools that provide innovative complex structures for designers and engineers to explore AM technology as well as analyze the material properties [14,15]. The material properties of functionally graded structures help determine the performance of the structure based on the constituent materials. Thus, it is important to develop feasible FGM design methods with materials gradients for specific material properties and performance.

The nature of living hinges offers one of the most intriguing uses of combined flexible and rigid FGM structures. Living hinges are examples of compliant mechanisms that consist of flexible members connecting two or more rigid members in regions with a desired range of motion. Common examples of living hinges include vice grips, crimping tools, bottles with caps, and binder clips with advantages such as minimized friction loss,

ease of fabrication, and ability to utilize small scale applications, among others [16]. By eliminating the traditional revolute joints in moving structures, living hinges use flexible regions to allow a specified range of motion in order to attain a desired performance.

Figure **1-4**: Example of a CAD model for a living hinge with a close-up view of the living hinge design.

The concept of design freedom and material complexity not only favors the production of multi-material additively manufactured parts, but also the development of such intricate structures using functional gradients. As mentioned, the PolyJet process produces precise and accurate parts from a range of composite materials. In order to achieve the desired material properties and quality of performance for manufactured functionally graded structures, the process of designing gradients with specific material compositions is crucial. Based on the versatility of the properties of functionally graded materials, living hinges can be designed and manufactured with a specified range of motion for a specific functionality depending on the design goals and criteria. The analogy of living hinge designs is constructively applied throughout this research work.

1.2 Research goals

Additive manufacturing has driven emerging design methodologies that allow designers to incorporate living hinges into new design applications. The use of multi-material AM has increased the opportunities for implementing functionally graded materials at the microstructural level to produce geometrically complex multi-material structures. The design freedom provided by the PolyJet process specifically, offers multi-material capabilities; however, it is rather difficult to identify and predict the mode of failure with different material properties. Incorporating multi-materials in living hinge designs increases adaptability for such designs hence increasing the ability to survive continuous loading conditions. Given the flexible nature of living hinges, the most common mode of failure is fatigue, which is a "rupture failure mechanism that results from the growth of cracks" according to the ASTM standard D4482-11 [17]. Fatigue usually occurs in parts with flexible material that are subjected to dynamic or fluctuating stresses after repeated cyclic loading causing the material to weaken.

The design approach process for functionally graded parts using the PolyJet process, based on the living hinge analogy, is critical as it encompasses analyzing different material compositions and structures that produce parts with desired range of motion. The ability to parse and understand the correlation between the design processes, structures, and behavior of living hinge parts designed with FGMs is important for engineers and designers within the AM community.

In order to better understand how gradient-based materials operate and how living hinge designs can be developed, this research work seeks to identify an efficient way to distribute material in different compositions and to improve the fatigue performance of functionally graded multi-material parts. The behavior of multi-material parts is analyzed by testing different multi-material gradient designs with varying lengths of material transition regions and flexible regions. Analyzing the fatigue life involves performing data statistical analysis for the independent and dependent variables selected due to a certain percentage of variance in the data caused by unforeseen circumstances in the experimental approach. The behavior of material gradients at the interface is additionally investigated. This information will help determine how fatigue life can be maximized and how the predictability of fatigue life in living hinges can be improved.

1.3 Thesis Overview

The research work presented in this thesis aims at analyzing the use of the PolyJet process to fabricate functionally graded structures, analyzing the quality of material gradients designed, and investigating the effects of the material gradients on the material properties, particularly the fatigue life of multi-material parts. In order to achieve the research goals mentioned above, the contents of the thesis are categorized as follows:

Chapter 2 focuses on the different methods of designing and manufacturing structures with FGMs. This chapter also highlights multiple research studies regarding process, structure, property, and behavior relationships of multi-material parts.

Chapter 3 describes the objective of the research, a summary of proposed research questions, an experimental set up, and the design procedures for three categories of functionally graded printed parts.

Chapter 4 provides pertinent information regarding the printing methodology as well as the fatigue and tensile testing procedures of all the functionally graded printed parts.

Chapter 5 provides detailed results and discussions for the fatigue and tensile testing procedures. In addition, the chapter summarizes the research findings through statistical data analysis.

Finally, Chapter 6 provides the implications and recommendations of the research study in addition to a summary and a conclusion of the research findings.

Chapter 2

LITERATURE REVIEW

2.1 Introduction

This chapter is divided into three sections presenting relevant research work that is related to designing and processing of multi-materials and functionally graded materials (FGMs). Section 2.2 presents existing literature that focuses on the design process of FGMs. Different studies are highlighted and compared for FGM design methodologies. Section 2.3 presents different methods and approaches undertaken to manufacture parts with FGMs using appropriate AM processes. Emphasis is placed on comparing the three known AM processes that are capable of processing multi-materials and FGMs. Finally, Section 2.4 presents the relationship between the process, structure, and behavior of parts manufactured by the material jetting process including summarizing related material properties.

2.2 Design of Functionally Graded Materials

The heterogeneous nature of FGM compositions causes non-uniformity in the material properties, which largely depend on the spatial position of the material across the bulk structure [18]. The spatial variation in the material composition of an FGM profile is achieved by gradually changing the volume fraction of the constituent materials during

the manufacturing process. The constituent materials are selected based on the requirements of their functional performance [19,20].

FGMs can be categorized into (1) continuous gradients or (2) stepwise or discrete gradients depending on their areas of application. Continuous gradients have smooth transitions in the material composition and microstructure with respect to the position within a structure. Stepwise or discrete gradients have discontinuities in their material compositions, which are due to the stacking of discrete layers of material while forming multilayered structures with immiscible compositions [21]. Since stepwise gradients have discretized regions of material compositions, delamination is prone to occur at the material interfaces under applied loads thereby affecting the material properties of gradient structures [22]. Figure 2-1 shows a stepwise or discrete gradient and a continuous gradient as well as a graph showing linear transitions to represent the continuous and discrete gradients. The smooth transitions between material compositions in continuous gradients are the underlying elements that inspire FGM designs.

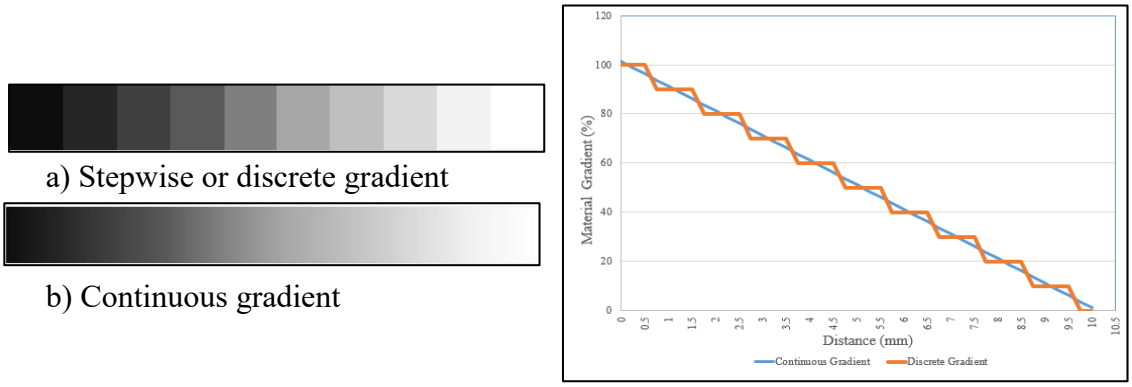

Figure **2-1**: Stepwise or discrete gradients (a) and continuous gradients (b) with accompanying gradient plots.

The ability to design functionally graded structures with either continuous or discrete gradients involves selecting appropriate materials and determining the optimal spatial variation for the composition of intended material phases. However, designing FGMs to successfully attain desired performance characteristics presents unique problems in terms of selecting appropriate compositions and material properties [23].

Several research studies have been performed using function-based representations of different models based on optimization and discretization methods to develop optimal FGM models with effective material properties. Doubrovski and co-authors [2] used mathematical expressions to create material gradients and voxel-based representations that define the microstructure, material, and the structural compositions of continuous gradients to develop functionally graded structures. Developing volumetric-based CAD tools are relevant for representing and designing heterogeneous models since such methods allow voxel by voxel definition of a material.

Research performed by Kawasaki and Watanabe [24] illustrates the use of simple functions with variable parameters and constraints to define and determine the spatial distribution of material in different constituent phases. Considering a function that changes discontinuously through a certain number of steps across a graded composition profile, the FGM forms a functionally graded structure with layers of material that differ in material composition. Tanaka and coauthors [25] provide an improved solution to specifically designing thermo-elastic materials with FGMs. Focusing on function-based representations to define the initial and boundary conditions for the material design

parameters, they designed materials by distributing the volume fraction. By way of numerous linear approximations, several iterations are required to reach an optimal state for the FGM model. Their form of FGM design is similar to several optimization methods that involve adjusting profiles of different spatially varied material compositions to develop more optimal FGMs. Further developing different paradigms of FGM design approaches, Markworth and coauthors [23] presented multiple modelling studies relative to designing FGMs. They noted that modelling of FGMs based on their microstructures permits the characterization of thermophysical properties because of the wide variety of microstructures that can exist across any graded direction.

A research study performed by Maciejewski and Mroz [26] is an example of how optimization methods can be used to create FGM design procedures for complex mechanical parts that undergo high loading conditions, both thermally and mechanically. Their example of creating an optimized FGM engine valve illustrates a numerical representation of the volume fraction distribution between a ceramic material phase within a metal matrix using mechanical and thermal constraints. Their proposed optimization method provides a practical design procedure for developing thermal resistant functionally graded structures with improved material properties such as low-wear surfaces and lightweight engine valves.

Existing CAD modeling methods have been explored to enable designers to create models with FGM variations that are easily transferrable to favorable manufacturing processes. Pratap and Crawford [27] present computer graphics techniques such as the

Volumetric Multi-Texturing (VMT) approach and hyper-texturing schemes to specify material composition values to the model's surfaces and blend them throughout the volume to create axial or linear directions of material gradients. They highlight that modeling a linear material gradient pattern starting with one material fraction and blending it with another material fraction can be achieved using multiple surface gradient functions depending on the structure. Huang et al. [28] applied the bi-objective optimization procedure to design functionally gradient materials. Analyzing the microstructures of primary materials, Tin (Sn) and an aluminum-based alloy 2124-T851, a micromechanical analysis method is used to develop effective material properties. By relating physical components at specific volume fractions and microstructures, effective material properties of FGMs can be obtained thereby developing advanced FGMs.

Furthermore, designing FGMs involves spatially varying the material compositions and using system type models for FGM design, processing, and performance. Other researchers have explored similar FGM design approaches. For instance, the systems approach demonstrated by Hirano and Yamada [29] used FGM design as an application to illustrate the "inverse design procedure" for a multi-paradigm expert system for engineering design. A systematic approach was taken by specifying the type of structure to be developed followed by selecting material compositions based on various assumptions for the spatially dependent material composition ratios. Other factors like thermal stresses and temperature distributions were determined using the material properties of various combinations until the most favorable conditions are achieved. A similar approach presented by Tanaka and coauthors [30], also Markworth [23] involved

using the optimization process in sequential steps to develop an optimal FGM design. The optimum composition profile of a FGM was not uniquely defined but rather comprised of various material properties that were selectively quantified for a desired application.

These research studies focus on identifying different functions of deriving a FGM; however, many researchers are looking into aspects such as direction and volume of the material gradient while developing optimal FGM designs. The goal in most research studies has been developing optimal FGM designs for structures with improved strength, lightweight, and minimized material usage. By using mathematical and function-based representations, different gradients of material have been derived. Dynamically combining compositions of materials ranging from metals, ceramics, concrete, polymers, to plastics and other forms of material composites has led to potentially creating structures with graded material properties.

Various design approaches and FGM applications have been presented with guaranteed manufacturability; however, the survivability of these FGM designs is not discussed or explored. Ongoing research aims at developing optimal FGM designs with compatible material properties. FGM design in AM relies on not only the availability of reliable design processes but also on the appropriate manufacturing capabilities that further support FGM processing.

2.3 Manufacturing of Functionally Graded Materials

Metallurgical processing methods such as jet solidification, slip casting, centrifugal casting, and powder stacking, among others have been used to develop FGMs with almost any material combination including metals, ceramics, and composites [31]. Furthermore, related studies by Mahamood and coauthors [32] have focused on developing FGMs using different processing techniques for metals. They comprehensively describe processing techniques of FGMs such as graded polymer processing techniques and melt processing in conjunction to well-established powder metallurgical techniques.

AM's contribution to the current state-of-the-art of FGM processing through material complexity and design freedom has led to the development of complex functionally graded structures. As discussed in Section 1.2, the material extrusion, DED, and material jetting processes are capable of processing multi-materials and possibly developing functionally graded structures. Whereas material extrusion is capable of processing multi-materials by simultaneously depositing layers of material extruded from two nozzles, the process does not have the ability to easily change the material composition during the manufacturing process.

Garland and Fadel [33] confirmed this aspect by using an off the shelf Fused Deposition Modeling (FDM)® (Stratasys Ltd., MN) 3D printer, the Big Builder printer™ (Builder 3D Printers, Netherlands), to show its ability to manufacture FGM parts as well as present the limitations thereof. Unlike the PolyJet process, the Big Build printer does

not allow the automatic change in composition during material deposition but rather requires that the first material is flushed out before extruding the second material. They found that 3.5 cubic millimeters of material was extruded when switching from one material to another. In addition, determining the optimal toolpath that would produce structurally robust functionally graded parts, especially in the XY direction is rather difficult to achieve. With that, the Big Builder 3D printer, is not suitable for manufacturing actual FGM parts but rather providing ideal FGM design visualizations and testing different toolpaths with different building parameters.

Conversely, the DED process has the capability to vary the composition of materials during its actual deposition, which allows the processing of FGMs. The key benefit of processing FGMs with the DED process as highlighted by Vaezi and coauthors [34] is the ability to implement gradual changes within the material composition during the deposition of powder and still achieve full density. The DED process has been explored by research pertaining to developing relevant processing techniques for end-use functionally graded metal parts. Shin and coauthors [35] particularly focused on the Laser Engineering Net Shaping (LENS) process to manufacture metal FGM parts. This process, as part of the DED process, allows the fabrication of functionally graded structures by varying the composition of the metal powder as it is being deposited into a laser beam melt pool. They designed a rectangular FGM part and varied the material composition from 100% copper to 100% nickel within the part's structure. Based on the analysis of the composition, each discretized region within the manufactured part had wide variability in the volume fraction of the material composition.

Comparably, the material jetting process has the ability to vary material compositions using jetted liquid photopolymers to finely control the compositions of materials for better quality FGMs. This is achievable through the simultaneous changing of the material composition in a prescribed toolpath during printing. The conformal behavior of functionally graded parts is dependent on the structural design and the material combinations. Researchers have looked into the processing of FGMs with the material jetting process. Bruyas and coauthors [36], for example, used the PolyJet process to design a multi-material compliant joint due to its ease of manufacturing intricate designs at the microscale level and the freedom of material choice. Even though current related research is limited in specifically addressing FGM processing using the material jetting process, most researchers have indicated that viable FGM processing methods are readily available. Deciding an appropriate processing method depends on the material gradient type, material compositions, and the geometry onto which the gradient is imposed.

Whereas research has shown that the material extrusion and DED processes are capable of processing multi-materials, the material jetting process dynamically mixes material compositions through drop-by-drop voxel-based deposition. In addition to the detailed design process of functionally graded structures, the behavior of functionally graded structures is critical in determining the compatibility of multi-material compositions and the resulting material properties. Based on the design and manufacturing capabilities of the material jetting process, it is important to develop in-

depth design frameworks that allow the manufacturing of functionally graded structures that achieve desired material properties.

2.4 Relating Process/Structure/Properties/Behavior of Material Jetted Parts

Related research mentioned in Section 2.3 highlights the relationship between the different manufacturing processes and their ability to develop functionally graded structures [37]. It is also important to understand the relationship between the material properties and the performance of different material composites in order to develop optimal FGM designs.

Various researchers have investigated the influence of several parameters such as orientation, material anisotropy, UV exposure, part aging, and surface finish, among others, on the mechanical properties of material jetted parts. For instance, research by Gay and coauthors [38] analyzed the variability of viscoelasticity as influenced by surface quality, orientation, and spacing of parts on the build tray. The surface quality of material jetted parts in the XY-orientation was not affected by the addition of extra layers during the printing process for a matte surface finish. Considering the geometry of a flat test parts, results showed that the viscoelastic behavior was significantly influenced by part spacing in the Y-direction compared to parts spaced in the X-direction that had no statistical significance. Parts manufactured in a 45° orientation had relatively lower viscoelastic behavior than those manufactured in an orientation parallel to the coordinated axis.

Focusing on the effect of build orientation on the material properties of material jetted parts, Barclift and Williams [6] found that the Z-orientation had a significant effect on the strength of parts and their dimensional accuracy. They also highlighted that over-curing of parts led to noticeable differences in the mechanical properties of manufactured parts. Similarly, Kesy and Kotlinski [39] studied the effects of build orientation on the tensile strength and hardness. They found that test bars oriented in the XZ-direction, along the direction of the build direction had higher hardness and density values. The weakest test bars had been oriented in the XY-direction. This was, in part, due to the light energy absorbed from the UV lamp along the edges than the layer surface.

Regarding material jetted test bars, Bass and coauthors [40] analyzed the characteristics of the anisotropic properties of six different material gradients with respect to the build orientation. They found that the test bars printed in the XY-orientation had higher tensile strength compared to the parts printed in the vertical, ZX-orientation. Increased concentration of TangoBlackPlus led to more elongation in the test bars printed in all orientations. Similarly, Pilipovic and coauthors [41] explored the properties of a variety of photopolymers such as VeroBlack™, FullCure720, VeroBlue™. Results showed that the FullCure 720 material had the maximum flexural strength compared to the other materials.

Besides other material properties such as tensile strength, hardness, and toughness, among others, fatigue is an essential material property required for the performance analysis of functionally graded structures. Failure in a structure caused by fatigue usually

occurs due to crack propagation within the structure. Fatigue characteristics of structures with rubber-like materials determine their expected lifespan after repeatedly applying dynamic loads. With time and multiple loading conditions, stress concentrations are introduced in the elastomers, which expands the cracks leading to complete failure [42]. This differs in metal and plastic components whereby the delamination of material between the build layers and the presence of internal crevices are the main contributors to premature fatigue failure [43,44].

Research done by Moore and Williams [45,46] focused on analyzing the fatigue life of material jetted specimens with TangoBlackPlus (TB+) and VeroWhitePlus (VW+) connected at a material interface in comparison to specimens with only TB+ material. The goal was to determine whether a multi-material interface was weaker than a single TB+ material. Preliminary results showed that at a mid-range extension of 40% elongation, 75% of the specimens with a material interface failed at the neck and had a higher fatigue life compared to the specimens with only TB+ material. This finding contradicted with their hypothesis; however, limiting TB+ material to the central region and VW+ on either end of the specimen, higher fatigue life was noted compared to both the TB+ and the single material interface specimens. Furthermore, TB+ material was used to analyze the relationship between fatigue life, location of failure, and elongation. Results showed that for decreasing strains, the expected fatigue life of TB+ increased thus the TB+ material had a more predictable fatigue life expectancy. Most of the variability experienced in the expected fatigue life was found to be due to recurring failure of the specimens at the material interface.

Whereas limited information currently exists regarding the fatigue characteristics of material jetted parts with elastomeric material properties and predicting the expected lifespan of elastomer components, these particularly research studies serve as a basis on which the fatigue life of TB+ material can be approximated. In order to produce effective functionally graded parts using the material jetting process, several mechanical properties such as tensile strength, hardness, stiffness, and fatigue have been explored to understand the relationship between the process, the structural quality of the parts and their overall behavior.

2.5 Scope of Research

Following the literature review on multi-material AM, it is noteworthy that prior research covers various ways of designing and processing FGMs. However, minimal research investigates the characterization of the material properties of parts printed with functionally graded materials, especially in fatigue. In order to address this gap, the primary focus in this research study is to investigate the effects of different material gradient types on the fatigue life of printed specimens.

Continuous and discrete material gradients with a constant volume of a flexible material, TB+, are compared. The goal is to determine whether a specific material gradient type or specific material transitions improved fatigue life of printed specimens. It is hypothesized that specimens with material interfaces of TB+ and a stiffer material would experience fatigue failure in the central region under cyclic loading. Furthermore,

continuous and discrete material gradients with a constant length of the flexible material are designed and fabricated to determine whether a consistent overall length of the flexible region increased or decreased the fatigue life of multi-material specimens. Lastly, the material properties of the specimens with different material gradients were compared to actual gradient compositions to show a correlation between the distribution of the material gradient transitions and the material properties therein. This research study helps determine whether or not having more material transitions in a specified material gradient transition region of the fatigue specimen improves the fatigue life properties of material jetted multi-material specimens.

Following Chapter 2, Chapter 3 presents the research methodology and in-depth design processes of the continuous and discrete material gradients for the categories of specimens with (1) a constant TB+ volume and (2) a constant TB+ length. In addition, the design process of specimens with individual material composites is discussed. Chapter 4 highlights the printing methodology as well as the fatigue and tensile testing procedures for all specimens designed. Chapter 5 presents the results obtained from the fatigue and tensile testing procedures as well as detailed discussions of the statistical analysis. Chapter 6 provides a conclusion of the research study and provides research implication and potential future considerations.

Chapter 3

EXPERIMENTAL APPROACH AND DESIGN METHODOLOGY

3.1 Research Methodology

With reference to the discussion in Chapter 2, multiple research studies have focused on developing FGM methodologies for relevant AM processes including the PolyJet process. However, functionally graded structures manufactured using the PolyJet process have no standard characterization of material properties; either mechanical, physical, or thermal. The variability of these properties can be determined through standardized tests that measure the non-uniformity of the materials in consideration with the nature and duration of the applied loads as well as the controlled environmental conditions [47].

The objective in this research, therefore, is to investigate the effects of different material gradient types and material transition lengths on the fatigue life of material jetted specimens for two instances: (1) a constant volume of a flexible material and (2) a constant length of flexible material. Fatigue specimens were designed with either continuous or discrete material gradients types dispersed in a region of specified length. The material gradients were implemented in order to demonstrate how each gradient type affects the expected lifespan of fatigue specimens. For each material gradient type, different concentrations of materials were selectively distributed over a specified length and the different material gradient transitions were analyzed. In summary, this research seeks to answer the following questions:

1. How does the length of the material transition within a specified region affect the fatigue life of multi-material PolyJet printed parts?
2. Will continuous material gradients offer a better advantage on the fatigue performance of PolyJet printed multi-material parts compared to discrete material gradients?
3. How are the properties of different material composites affected by the individual materials in their compositions when a color-based dithering approach is used?

For this research, it was hypothesized that as the length of the material gradient transition region increased linearly, the distributed material properties within the specimen would improve fatigue life. In addition, the fatigue life was expected to improve as the material gradients within the specimen accurately converged to an ideal continuous linear gradient pattern. The work presented herein helps determine whether or not varying material over a specified length improves the fatigue life of specimens printed with different material gradients.

Following in this chapter, Section 3.2 presents the design procedure of the fatigue specimens and the design of experiments approach. Sections 3.3 and Section 3.4 present in detail the individual design processes for the fatigue specimens with continuous material gradient and discrete material gradients respectively. Section 3.5 presents the design process of specimens with individual material gradient percentages as an additional analysis of material properties of multi-material specimens.

3.2 Experimental Design Procedure

In order to analyze the fatigue life of multi-materials, fatigue specimens were designed according to the ASTM D4482-11 standard [48] as shown in Figure 3-1. The fatigue specimens were designed to be tested in tensile-strain cycles. Since most traditional specimens can easily detach from the grips due to the lateral shrinkage present when under high loads and strains, additional round-beaded edges were designed around the edges of the specimen. An extended length to the grip region was also added in order for the specimens fit securely into a set of special grips during fatigue testing.

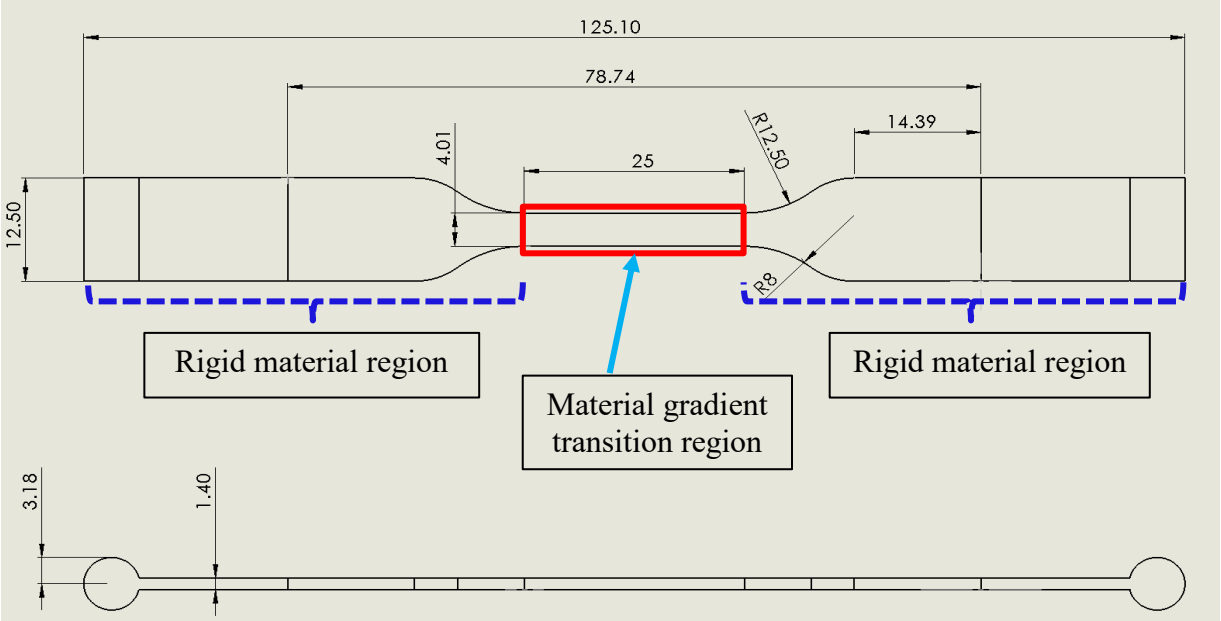

Figure **3-1**: A CAD model of a specimen. All units are in millimeters.

The analogy of a common living hinge design was considered for all specimens whereby a flexible material, TangoBlackPlus (TB+), was defined along with a series of material gradients dispersed over a length of 25mm in the material gradient transition

region of the specimen. By distributing gradients of materials within a specified region for a desired deflection and an optimal range of motion, the considerations for common living hinge designs were emphasized. In addition to common living hinge designs, material gradients can be applied to multi-material lattice structures as well structures with metal composites for a desired level of material complexity.

A design of experiments was used to ensure a systematic fatigue testing procedure. For this reason, two analyses were considered: (1) a constant TB+ volume and (2) a constant length of TB+ in the material gradient transition region for all specimens designed with continuous and discrete material gradients. The independent and dependent variables considered for this research study are presented in Table 3-1. Figure 3-2 shows a flowchart that helps to illustrate the experimental design based on the experimental constant variables.

Table **3-1**: Presents the variables selected for this research study.

Variables	***Parameters***
Constant	Volume of TB+/ Length of TB+
Independent	Length of the material transition
	Continuous and discrete material gradients
Dependent	Fatigue life and Failure location

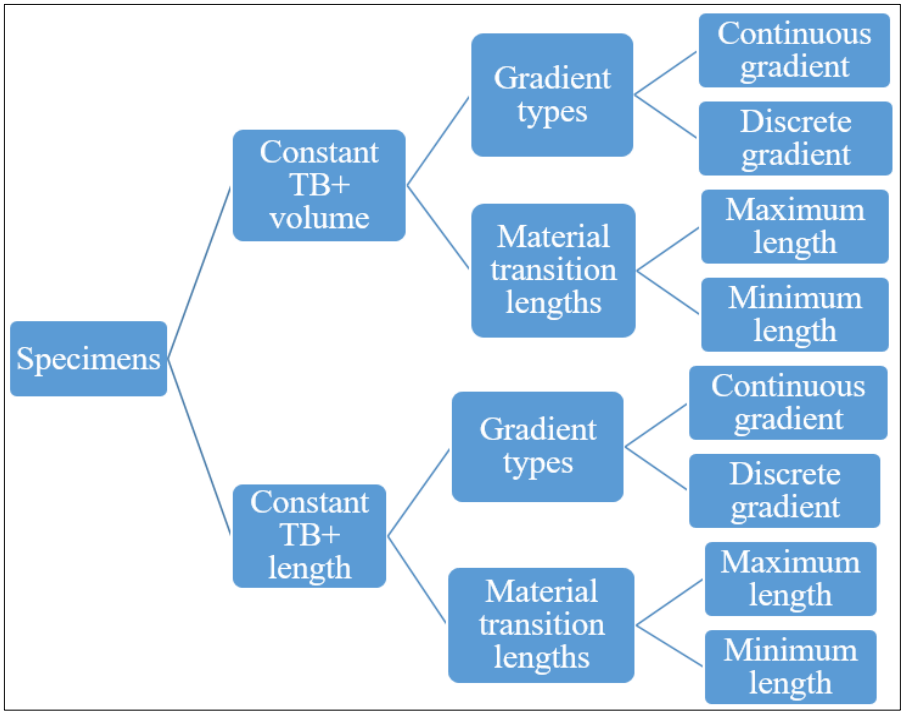

Figure **3-2**: A flowchart that highlights the experimental design approach.

Control specimens, also used as the base control specimens, were designed such that the material gradient transition region had a dual multi-material interface comprising only a rigid material, VeroCyan (VC), and a flexible material (TB+) instead of a distribution material gradients. As the base control specimens, the length of TB+ material in the control specimens was particularly used to calculate the constant volume of TB+ used for specimens with continuous and discrete material gradients. In addition, the total length of the TB+ material, 13.69 mm, in the control specimens was used as the fixed length for specimens with continuous and discrete material gradients. The main reason for considering fatigue specimens with a constant volume of TB+ was to analyze whether the predictability of failure and changing the distribution of material gradients within a specified region could improve the fatigue life. Also, a constant length of TB+ material

was considered so as to analyze the fatigue life of specimens with a specific flexible region in addition to the material gradients in the transition region.

In order to test the effectiveness of mixing the VC and TB+ materials, the material transition region in the central region was divided into two lengths in a linear transition pattern. A shorter length, denoted as the minimum length or min-length, had a diminished material transition length whereas the larger length, denoted as the maximum length or max-length, maximized the transition region to the entire length of the material gradient transition region. Fatigue specimens with either maximum or minimum material transition lengths were designed for continuous or discrete material gradients to be applied and were tested under similar fatigue testing conditions.

3.3 Design Process for Continuous Material Gradients

In order to develop the material gradients based for the proposed experimental approach, in-depth design processes were developed and are described in detail in Sections 3.3 and 3.4. To begin with, the design process for the continuous material gradients is summarized in the flow chart shown in Figure 3-3. The process comprises a part geometry track and a material geometry track both of which contribute to the generation of continuous material gradients when combined.

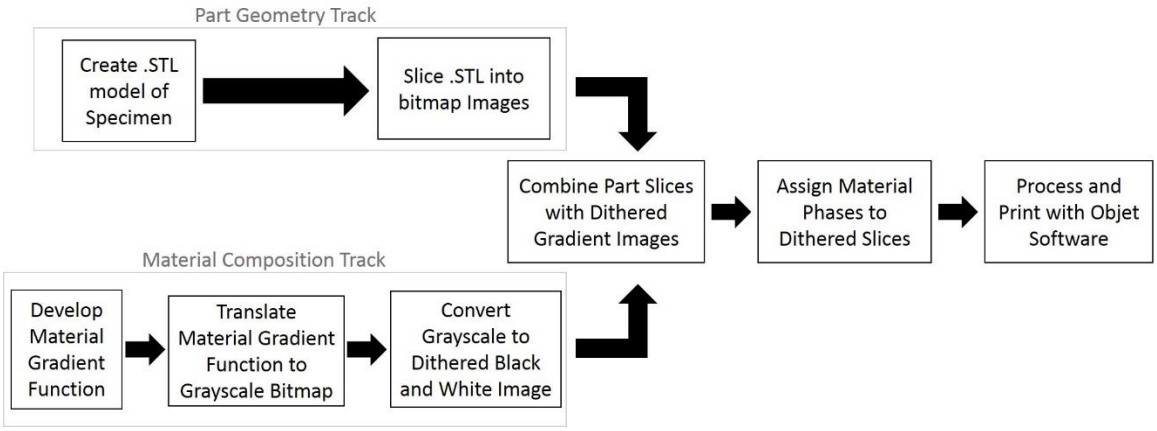

Figure **3-3**: Flowchart showing the systematic design process of the continuous material gradient specimens.

For the material composition track, the continuous material gradients were created from equations of functions that were formulated based on the simplest form of gradients that would describe a systematic gradual transition of material within the material gradient transition region of the specimen. Figure 3-4 presents a graph with three plots displaying the linear pattern for the maximum and minimum material transition region compared to that of the base control specimens highlighted by the blue line. These plots were generated for specimens with continuous material gradients and a constant volume of TB+. The volume of TB+ was dispersed linearly across the surrounding area to create a smooth linear material transition between the rigid and flexible materials. A sharper incline in the length represents a shorter material transition region thereby implying a longer fully flexible region. The length of the material gradient transition region represented by the plots in Figure 3-4 and Figure 3-5 is the 25mm, the material gradient transition region of the specimen.

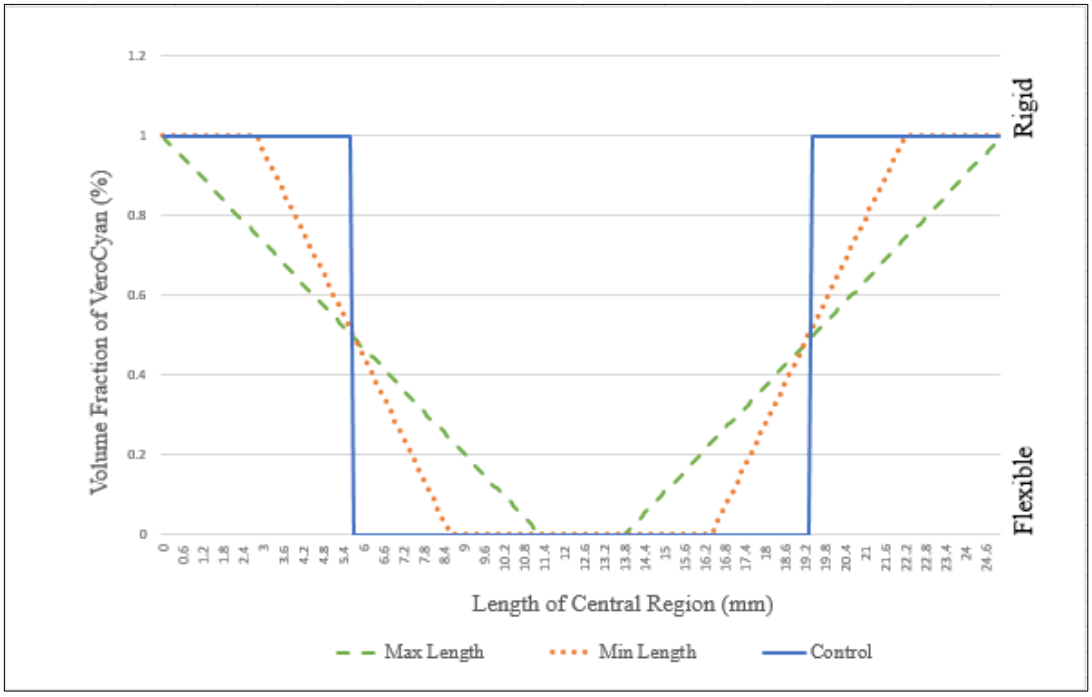

Figure **3-4**: Plot showing the maximum and minimum material transition lengths in relation to the material transition of the control specimens for a constant TB+ volume.

Similarly, Figure 3.5 presents a graph with plots showing the linear pattern for maximum and minimum material transition region compared to the linear pattern of control specimens. However, these plots were generated to represent continuous gradient specimens with a constant length of TB+ in the material gradient transition region.

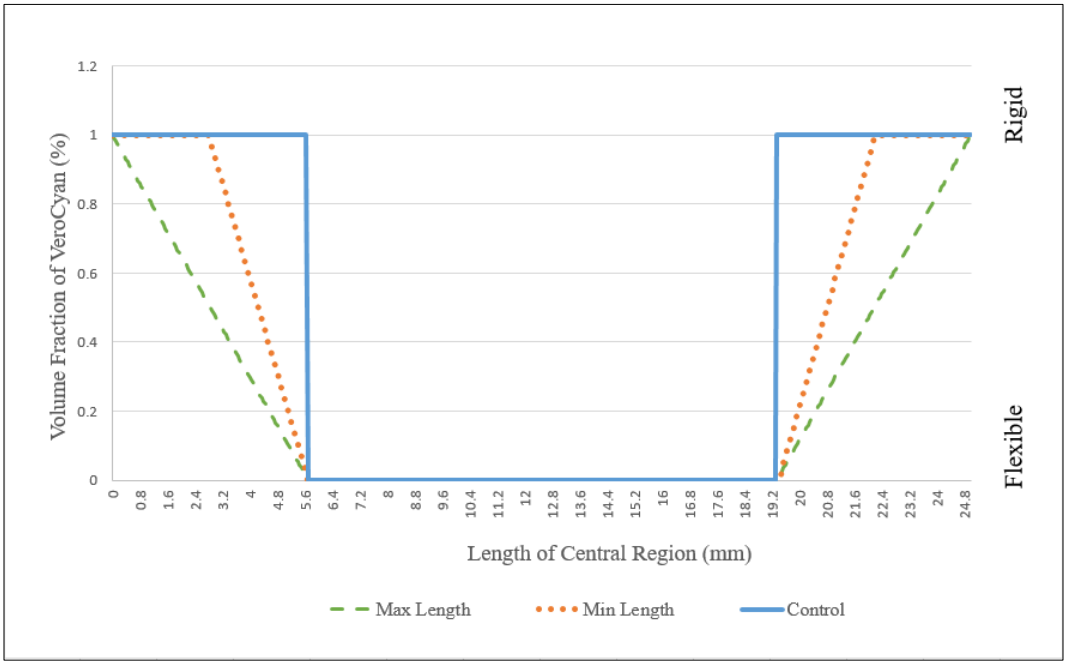

Figure **3-5**: Plot showing the maximum and minimum material transition lengths in relation to the material transition of the control specimens for a constant TB+ length.

For either graph, the maximum and minimum material transition lengths are plotted along with the base control specimens in order to show the variation between the material gradient for each gradient type over the same specified length. The plot ranges from 0 to 1 for the volume fraction of the rigid material, VeroCyan (VC), implying the rigidity for values closer to 1 or flexibility for values closer to 0. Analyzing the different material transition lengths allows the evaluation of properties such as strength, stiffness, toughness, and durability of printed parts with similar distribution of material.

The equations of functions were used along with an in-house MATLAB® code (The MathWorks, Inc., MA.) to create grayscale bitmap images as shown in Figure 3-6.

Figure **3-6**: Grayscale gradient images: max-length (top) and min-length (bottom).

The Floyd-Steinberg error diffusion algorithm [49] uses an error diffusion technique to generates an error for each pixel and distributes it to other surrounding pixels in an image. In addition, the algorithm can increase the resolution of apparent colors in images by dithering where grayscale images are converted to binary images. For this reason, the algorithm, as commonly used in MATLAB, converted the grayscale images shown in Figure 3-6 to dithered binary images with only black and white pixels in bitmap format shown in the Figure 3-7.

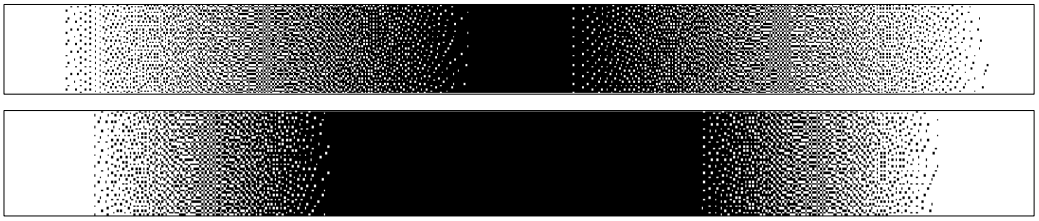

Figure **3-7**: Dithered binary images showing a linear pattern of material transitions for specimens with a constant TB+ volume: max-length (top) and min-length (bottom).

Following the material geometry track, the part geometry track consisted of an STL file obtained of the specimen CAD geometry shown in Figure 3-1. Autodesk® Netfabb® software (Autodesk, Inc., CA) was used to create a series of individual slices saved in bitmap (.BMP) format of the STL file. Figure 3-8 shows examples of .BMP mask images that defined the external geometry of the specimens were obtained from the STL file.

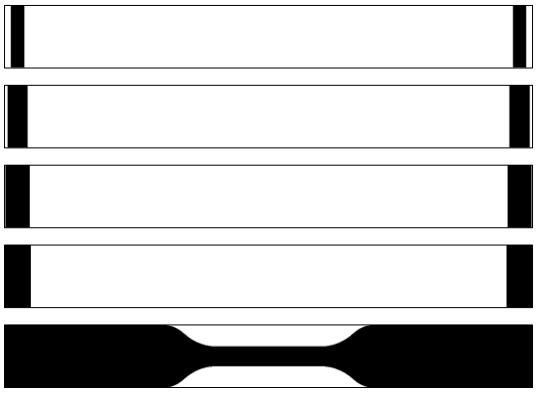

Figure **3-8**: Examples of .BMP slices generated with the Autodesk® Netfabb® software.

The combination of the individual .BMP slices from the slicing software and the dithered bitmap images from the gradient function within the in-house MATLAB code resulted into combined images as shown in Figure 3-9, specifically for .BMP slice 087.

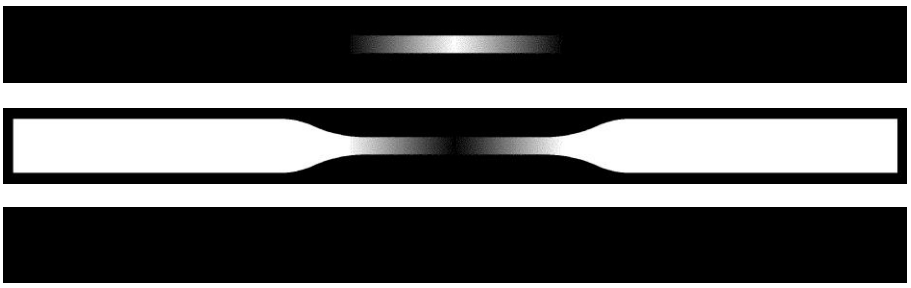

Figure **3-9**: Examples of bitmap slices showing combined images of specimens with constant TB+ volume including material assignments for TB+ (top), VC (middle), and VeroZ (bottom) materials.

For each combined image, a total of 245 bitmap slices were generated with a uniform layer thickness of 0.030 mm. For each bitmap slice, three materials were assigned in accordance with the printing parameters with two primary materials, TB+ and VC. The third material, "VeroZ" was only added so that during the printing process, the number of bitmap slices are identical for all material assignments. As illustrated in Figure 3-9, the binary format relates 0 to black and 1 to white. This implies that for each material

assignment, a specific material is present or “on” and therefore deposited if the bitmap slice has a white-shaded region. Likewise, if the bitmap slice has a black-shaded region, then it implies that a specific material is not present or “off” and therefore not deposited. Since only two materials were required for the specimens, the resulting bitmap slices with a VeroZ material assignment contained all zeros hence a black-shaded region. Figure 3-10 shows examples of specimens fabricated with the continuous material gradient applied within the central region as a result of this specific design approach.

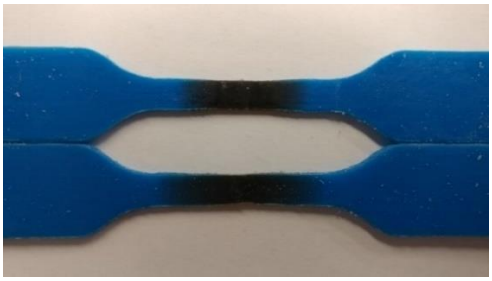

Figure **3-10**: Printed specimens showing continuous material gradient applied to the central region: min-length (top) and max-length (bottom).

3.4 Design Process for Discrete Material Gradients

The design process of the discrete material gradients was similar to that of the continuous material gradients in such a way that gradient functions were developed based on non-continuous discrete functions. The flowchart shown in Figure 3-11 represents the systematic procedure considered for developing discrete material gradients.

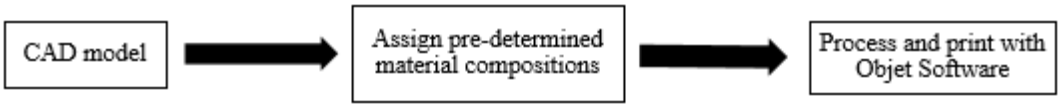

Figure **3-11**: Flowchart showing the systematic design process of the discrete material gradient specimens.

The material gradient transition region of the fatigue specimen CAD model was partitioned into sections with different lengths onto which the different material gradient concentrations were applied. The gradient percentage concentrations of TB+ material were selected from a compilation of out-of-the-box percentages as pre-established by Stratasys® (Stratasys, Inc., MN). The examples of pre-established gradient concentration percentages shown in Table 3-2 can be naturally handled by the PolyJet process.

By comparing the maximum and minimum lengths of the material gradient concentrations, it was possible to determine whether a difference in material properties at each interface affects the fatigue life of the specimen.

Table **3-2**: Material concentration percentages used for the discrete gradients at maximum and minimum lengths.

Lengths	*Percentages of TB+ material*
Max-Length	10%, 25%, 65%, 80%
Min-Length	25%, 65%

Figure 3-12 presents a graph comparing the maximum and minimum material transition length in the material gradient transition region to the material transition of the control specimens. The plots display uniform stepwise transitions between different volume fractions of the rigid material. Like Figure 3-4, the plot also ranges from 0 to 1 for the gradual material transition, which implies the rigidity of the material for values

closer to 1 or the flexibility of the material for values closer to 0. Using this graph, the material compositions used for the discrete material gradients were determined for each section. Likewise, the length of the material gradient transition region represented by the plots in Figure 3-12 and Figure 3-13 is the 25mm, the material gradient transition region of the specimen.

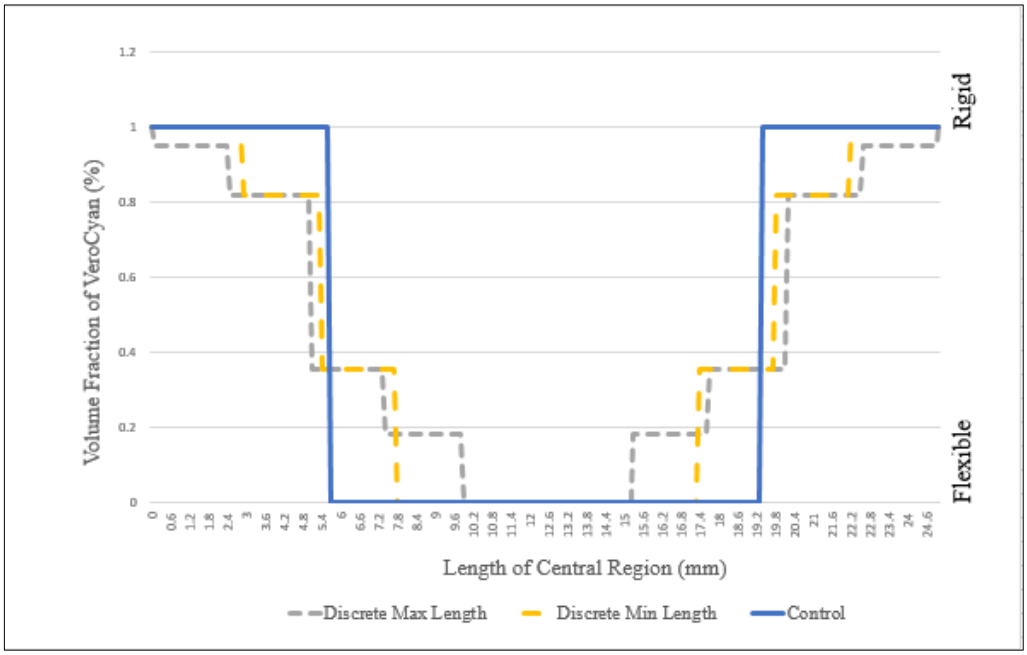

Figure **3-12**: Plot showing the maximum and minimum lengths of the discrete material gradients in relation to the material transition of the control specimens for a constant TB+ volume.

Similarly, plots were generated to represent discrete material gradient specimens with a constant TB+ length as shown in Figure 3-13. The graph presents plots showing the maximum and minimum material transitions region compared to the transition in base control specimens.

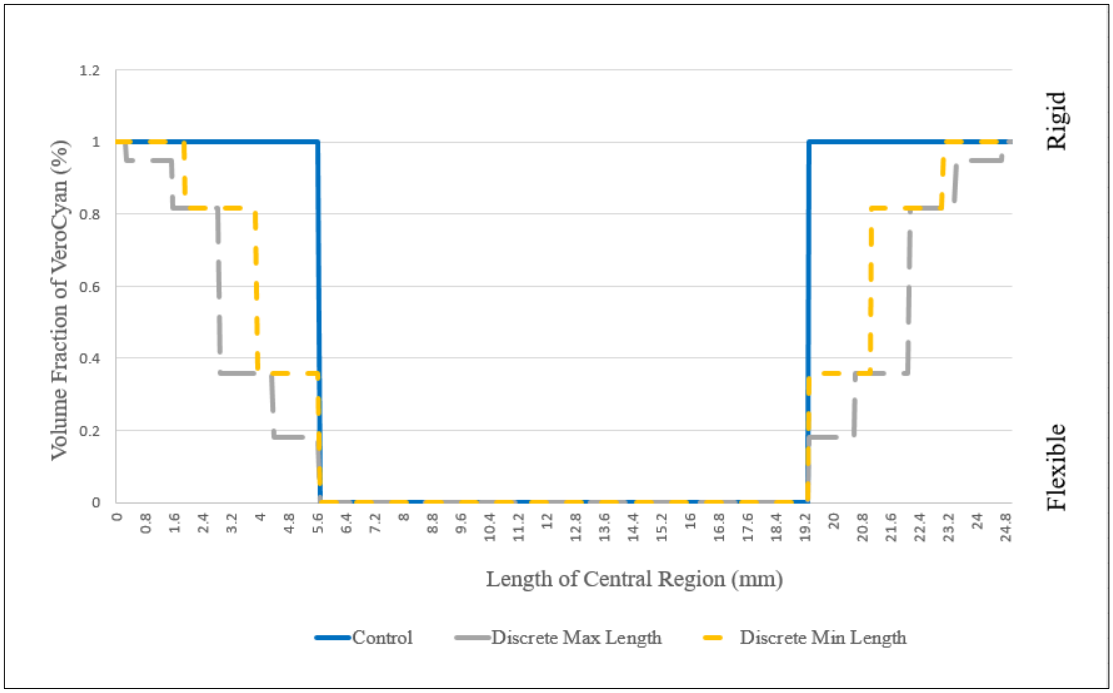

Figure **3-13**: Plot showing the maximum and minimum lengths of the discrete material gradients in relation to the material transition of the control specimens for a constant TB+ length.

Stock material concentrations from Stratasys® were used to create discrete transition regions with interfaces every 2.45 millimeters. The gradient concentrations were also used to recreate the transition region with the continuous gradients, which stretched across the same length of region. A SolidWorks rendering of a specimen with discrete material gradients is shown in Figure 3-14 and a final printed specimen showing the discrete material gradients is shown in Figure 3-15.

Figure **3-14**: SolidWorks rendering of a CAD model with sections of discrete gradients.

Figure **3-15**: Printed specimen showing the discrete material gradient in the central region.

3.5 Design Process for Specimens with Individual Material Composites

Besides analyzing continuous and discrete material gradients, the goal for analyzing individual material composites was to determine whether the relationship between the material properties reflected the relationship between the different material compositions. The design process of specimens with individual material composites was similar in approach to the design process of the continuous material gradients as demonstrated by the flow chart in Figure 3-3. The difference between the continuous material gradient and the individual material composites is that the material gradient was not localized to the material gradient transition region but rather applied throughout the entire specimen.

Individual material composites were selected based on a desired percentage of rigid material uniformly distributed throughout the specimen. The material compositions selected ranged from 0% to 100% of the rigid material. Figure 3-16 shows examples of printed specimens with different material compositions.

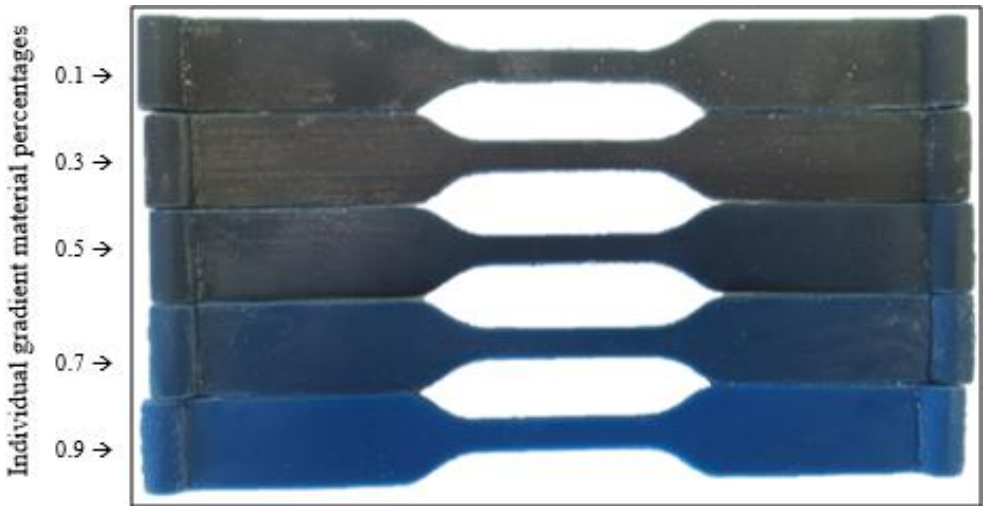

Figure **3-16**: Printed specimens showing individual material composites with increasing percentages, from top to bottom, of the rigid material, VC.

As shown in the Figure 3-16, an individual material composite of 0.1 implied that the specimen was composed of 10% rigid material and 90% flexible, TB+ material. In order to analyze the material properties of specimens with each material composite, a tensile testing procedure was performed. The independent and dependent variables considered for this analysis were the composition of the flexible material, TB+ and the maximum tensile stress respectively.

In the next chapter, Chapter 4, the printing methodology is described in detail. The fatigue and tensile testing procedures for the specimens with a constant volume, a constant length, and with individual material composites is discussed in detail respectively.

Chapter 4

PRINTING METHODOLOGY, FATIGUE AND TENSILE TESTING PROCEDURES

The printing methodology for the specimen groups with continuous and discrete material gradients, as well as specimens with individual material composites, is discussed in Section 4.1. The fatigue testing procedure is divided into Sections 4.2.1 and 4.2.2 to describe the fatigue testing procedure for specimens with constant TB+ volume and specimens with constant TB+ length respectively. Section 4.3 provides the details of the tensile testing procedure for the specimens with individual material gradient percentages.

4.1 Printing Methodology and Specifications

All specimens were fabricated using the Objet350™ Connex3™ (Stratasys Ltd., MN) PolyJet printer with VeroCyan (VC) and TangoBlackPlus (TB+) as the model materials. The ideal build orientation of the specimens on the build platform was the XY orientation [5] because it ensures a single pass of the print head per layer of material deposited. The XY orientation is also important because the printed specimens received uniform curing of the deposited material through the uniform exposure of UV light during the printing process. All specimens were printed with TB+ material with one UV lamp active during printing based on the default settings. This was to ensure that the TB+ regions of the specimens were not over cured. The surface finish was set to “matte” to ensure uniform surface finish effects across all printed specimens. Table 4-1 provides a summary of additional process parameters of the Objet350 Connex3 PolyJet printer.

Table **4-1**: Process parameters for the Objet350 Connex3 PolyJet printer.

Process Parameter	***Specifications***
Temperature	Print heads: 65-72°C Ambient temp: 32°C
Build time	Discrete gradients: ~3 hours per build tray Continuous gradients: ~ 1 hour per specimen
Layer thickness	0.030 mm
Printing Mode	Digital materials mode

Objet Studio™ (Stratasys Ltd., MN), a server software, was used to prepare all specimens for printing since it effectively supports STL files in making high quality and accurate models. Specimens with the discrete material gradients required manual selection of predetermined digital stock material concentrations provided by Stratasys® with a variety of material combinations of the model materials based on the corresponding gradient concentration percentages. Specimens with the continuous material gradients as well as with the individual material composites were fabricated using the Voxel Print software also supplied by Stratasys®. The software used the dithered bitmap slices to specify the material composition of the specimen at the voxel level. Individual bitmap slices were printed in the digital materials (DM) mode. The print resolution was set to 600dpi for the X-axis and 300 dpi for the Y-axis. During voxel printing, one specimen was printed at a time for an average printing time of about 54 minutes each.

Support material, FullCure SUP705, is mandatory in the PolyJet process and it was jetted simultaneously along with the model materials through separate print head nozzles. Support material offers stability and minimizes premature failure, especially for regions with the TB+ material. Due to the delicate nature of the printed specimens especially in the central region with TB+ material, support material was removed by water jetting at

low pressure. All printed specimens were cleaned of all support material and stored in a dry place prior to any testing procedures.

4.2 Fatigue Testing Procedure

Based on the ASTM standard D4482-11 [48], the fatigue testing procedure evaluates the ability of parts with elastomeric components to resist dynamic cycling fatigue. The significance of using this ASTM standard test method was that the fatigue data obtained would provide an estimate of the crack initiation behavior, the fatigue life of the tested parts, and the behavior at the multi-material interface. The following sections describe the fatigue testing procedure for the specimens with constant TB+ volume and constant TB+ length.

4.2.1 Specimens with constant TB+ volume

Fatigue testing of specimens with a constant TB+ volume involved measuring the number of cycles to failure for the complete rupture of the specimens under repeated cyclic loads. The printed specimens were mounted onto the MTS 880 Servo hydraulic material test system shown in Figure 4-1.

Figure **4-1**: The MTS 880 Servo hydraulic Material Test System (left) and the non-compression grips and a sample specimen (right).

This testing system was selected because of its capability of handling small loads, a wider frequency range, and a large extension range as described in the ASTM standard. The specimens were tested for fatigue in loading and relaxation cycles under displacement control at a fixed frequency of 1.7Hz with a period of 0.588 seconds. For each testing cycle, an extension of 40% elongation 40% of the total length of TB+ material in control specimens, a length of 13.68mm, was used. One cycle was measured starting from the rest position at zero extension to the position at maximum extension. The standard also specifies that the specimens are tested with four phases of equal length: i) hold at zero extension, ii) ramp linearly upwards from zero extension to maximum extension, iii) hold at the maximum extension, and iv) ramp downwards from the maximum extension to zero extension. Failure in all specimens was when the specimens completely ruptured.

Based on the design of the specimens, mechanical grips were deemed necessary to fasten the specimens to the load cell and the load frame. For this, two special grips made out of aluminum blocks were machined with M6 x 1 bolt taps drilled and slots cut through. For each grip, an additional hole was drilled above the slot so that the beaded edge of the specimen would snugly slide through it. The slots were cut to snugly fit the thickness on either end of the specimens. One grip was attached to the actuator whereas the other grip was fastened to the base of the load frame also shown in Figure 4-1. A total of 15 fatigue specimens with a constant volume of TB+ were tested. The parameters tabulated and recorded included number of cycles to failure and the maximum load at failure. Failure location was analyzed subsequently.

4.2.2 Specimens with constant TB+ length

Similarly, fatigue testing of specimens with a constant TB+ length provided the number of cycles to failure for all specimen groups. Fatigue tests were performed on the Instron 5866 mechanical test system onto which specimens were mounted. The Instron 5866 test system is commonly used as a tensile testing machine; however, the ASTM Standard [17] supports the use of the machine as an alternative. The maximum cross-head speed of the test frame is 20in/min, which is equivalent to 8.47mm/sec.

For the fatigue tests performed, pneumatic grips shown in Figure 4-2 were used instead of standard mechanical grips. Pneumatic grips were attached to an air pressure source, which was set to about 60psi prior to testing for a snug tight gripping of the specimens.

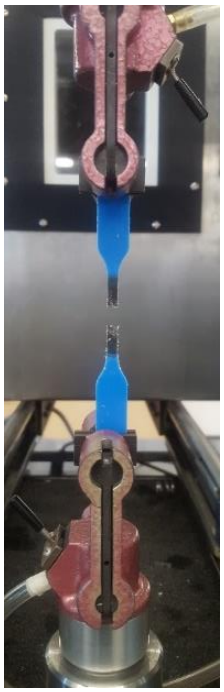

Figure **4-2**: Fatigue testing with the Instron 5866 Mechanical Testing System showing a failed specimen.

For each testing procedure, the test system was set to a speed rate of 40%/sec, which is approximately 5.47mm/sec based on an elongation of 40% of the total length of the region with TB+ material in control specimens, a length of 13.68mm. Based on the delicate nature of the specimens, a 100 N load cell was used due to its ability to handle small loads. The test frame was set to run up to 2000 cycles and was promptly stopped at the complete rupture of each specimen tested. A total of 25 fatigue specimens with a constant length of TB+ were tested and the parameters recorded included number of cycles to failure and the maximum load at failure. Failure location was also analyzed subsequently.

Two different mechanical testing systems were used for fatigue testing due to the availability of facilities with dissimilar testing equipment. Although all fatigue specimens were tested under similar tensile-strain loading conditions at a uniform maximum extension, the waveform shape and the loading rates at which the machines run were slightly different to accommodate the different test frames. As a result, the number of cycles to failure for the fatigue specimens tested may be impacted.

4.3 Tensile Testing Procedure

According to the ASTM standard D638 [50], the significance of performing tensile tests is to determine the mechanical properties of standard test specimens. In the case of the specimens fabricated with the individual material composites, tensile tests were performed in order to analyze their mechanical properties in relation to the specific material compositions based on color. Tensile testing was performed with the Instron 5866 Mechanical Testing Machine using mechanical grips as shown in Figure 4-3.

Figure **4-3**: Tensile testing with the Instron 5866 Mechanical Testing System.

Four groups of specimens with individual material composites were designed ranging from 20% to 80% rigidity. Three specimens were tested within each group under continuous loading conditions in tension at a fixed rate of 40%/sec, which is equivalent to 5.47 mm/s. The parameters recorded included the maximum tensile stress, maximum load, and extension at break.

Chapter 5

RESULTS AND DISCUSSION

5.1 Data Analysis for Specimens with Constant TB+ Volume

Chapter 4 elaborated on the experimental approach, printing methodology, and the fatigue and tensile testing procedures of all specimen groups. This section provides detailed analysis and discussion of the results obtained for specimens with a constant TB+ volume. This analysis explains the fatigue performance of the material gradients at different material transition lengths. Table 5-1 presents the results obtained from the fatigue testing procedure discussed in Section 4.2.1.

Table **5-1**: Data obtained for fatigue tested specimens with a constant TB+ volume.

Material Gradient Types	*Lengths*	*No. of Specimens*	*Cycles to Failure*	*Failure Location*
Continuous Gradients	Max-length	Specimen – 1	10	TB+ and Transition Gradient Interface
		Specimen – 2	11	TB+ Region
		Specimen – 3	35	TB+ Region
	Min-length	Specimen – 1	1077	TB+ and Transition Gradient Interface
		Specimen – 2	895	TB+ Region
		Specimen – 3	739	TB+ Region
Discrete Gradients	Max-length	Specimen – 1	292	TB+ Region
		Specimen – 2	693	TB+ Region
		Specimen – 3	157	TB+ Region
	Min-length	Specimen – 1	627	TB+ Region
		Specimen – 2	2001	No Failure
		Specimen – 3	2001	No Failure
Control Specimens		Specimen – 1	2001	No Failure
		Specimen – 2	2001	No Failure
		Specimen – 3	2001	No Failure

The data was analyzed for statistical significance using two-way analysis of variance (ANOVA) in SPSS® (IBM Corporation, NY) using the IBM SPSS Statistics software. Two-way ANOVA was used in order to determine the main and interaction effects of different material gradient type and gradient lengths with respect to the number of cycles to failure. All the assumptions made for using two-way ANOVA to analyze the data were met accordingly except for the homogeneity of variance test performed in SPSS®, which was not met since $p < 0.05$. However, ANOVA is generally robust against violations of homogeneity of variance when sample sizes are equal; so, statistical analysis was still conducted. The two-way ANOVA tests showed a statistical significance between the continuous and discrete material gradients with a p-value of 0.047 as well as the maximum and minimum lengths with a p-value of 0.001. The interaction, however, between the gradient types and the maximum and minimum lengths showed no statistical significance since $p > 0.05$.

The input data statistically analyzed and reported contained outlying data points for the number of cycles to failure. These points were not excluded since the number of specimen samples was small (15 specimens) and a two-way analysis of variance tests requires that all groups compared have equal number of samples. The outlying data points might have been caused by different aging effects, varying humidity levels, and inconsistent fatigue test setup for the different specimens groups.

Table **5-2**: Statistics obtained from the fatigue testing procedure of specimens with a constant TB+ volume.

		Fatigue life (# of cycles to failure)	
Material Gradient Types	*Lengths*	*Mean*	*Standard Deviation*
Continuous Gradients	Max-length	18.67	14.2
	Min-length	903.67	169.2
Discrete Gradients	Max-length	380.67	278.8
	Min-length	1543.00	793.3
Control Specimens		2001	0

In order to compare the main effects between different group interactions, the Tukey test, a post-hoc statistical analysis test in SPSS®, was used to perform multiple comparison procedures between different groups. Comparing both material gradient types to the control specimens, the Tukey test showed a statistically significant difference. Similarly, there was a statistically significant difference observed when control specimens were compared with the maximum and minimum lengths of the material transition regions for both material gradient types.

To further understand how fatigue life varied among specimens groups with different lengths of regions with 100% TB over a constant volume of TB+, Figure 5-1 presents a plot showing this variation. In the plot, it is clearly seen that any specimens with a minimum length of material gradient transitions, also denoted as Continuous-Min and Discrete-Min, had higher number of cycles to failure than their counterparts, the specimens with a maximum length of material gradient transitions. The control specimens out-performed the specimens with either continuous or discrete material gradients with a

higher fatigue life since they had the largest amount of flexible material distributed in the material transition region.

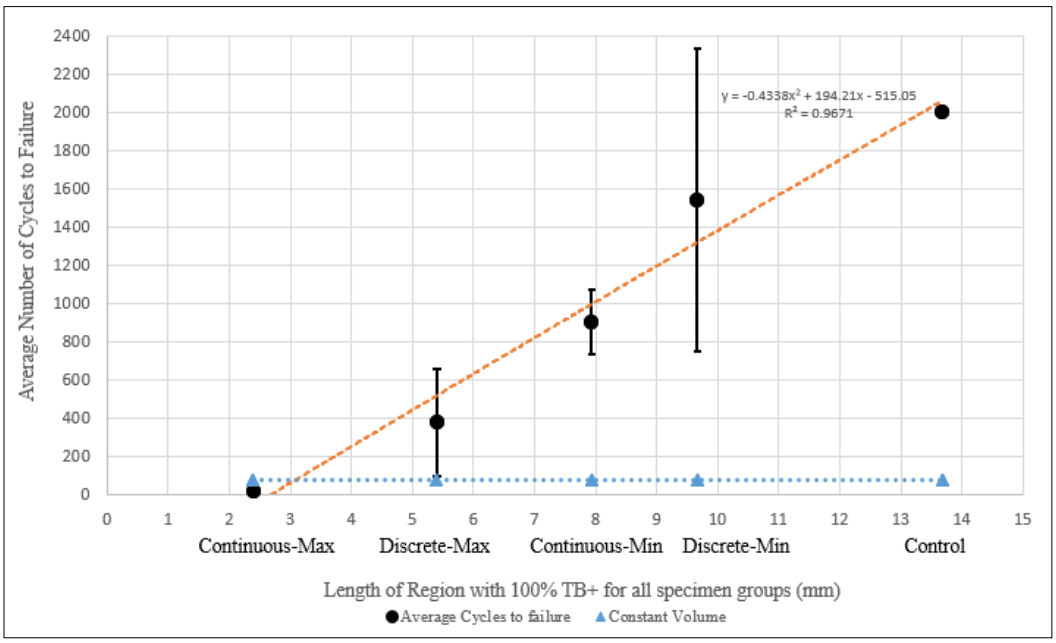

Figure **5-1**: The average number of cycles to failure with the standard deviations error bars based on the regions with 100% TB+ for all specimens tested.

Comparing the average number of cycles to failure for each specimen group as shown in Figure 5-2 also shows similar variations. It was hypothesized that as material was more evenly distributed in the material gradient transition region, the addition of material compositions would offer an improved fatigue life and more reliable locations of failure; however, specimens with a maximum length of material gradients had a lower fatigue life compared to specimens with a minimum length of material gradients. This is due to uneven distribution of material caused by maintaining the volume of TB+ in the material gradient transition region. In addition, since the specimens were tested for fatigue at a

constant strain, the weakest material, that is the flexible material with a shorter length, experienced higher stresses which caused premature fatigue failure.

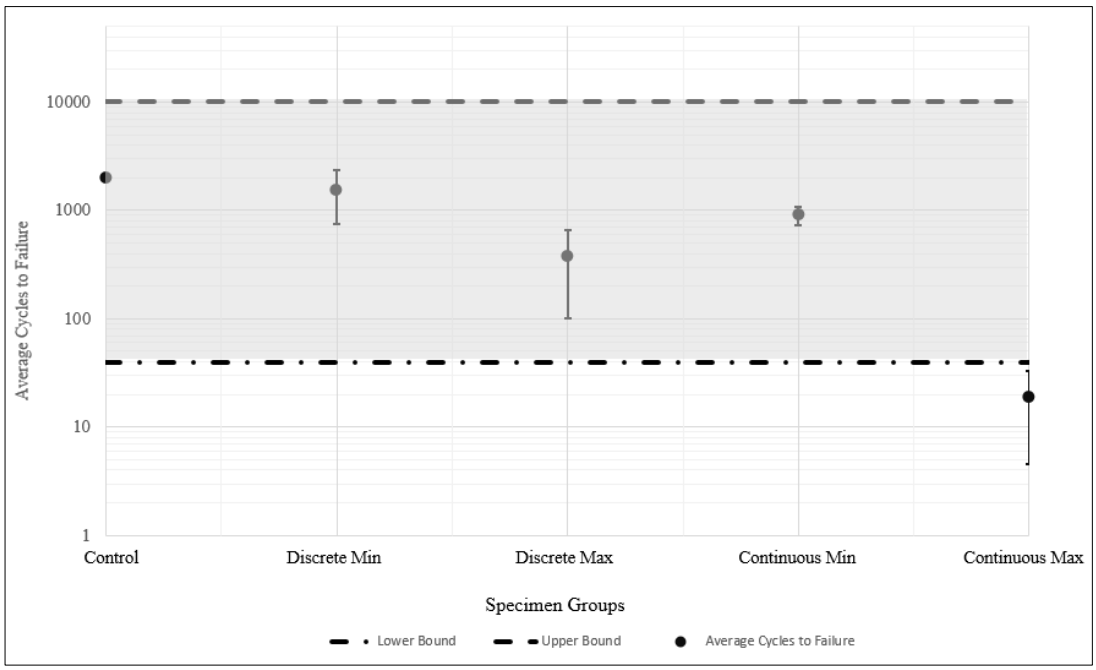

Figure **5-2**: The average number cycles to failure with the standard deviations error bars compared against all specimen groups tested.

As previously discussed, one of the key questions targeted by this research was whether the use of gradient material transitions can avoid the unpredictable failure at the material interface as observed in previous studies by Moore and Williams [46]. However, the premature interfacial failure was not observed in initial testing, potentially due to the small number of specimen replications for each condition. The shaded grey region shown in Figure 5-2 denotes the 95% confidence interval established by Moore and Williams at the 40% elongation, which allows this present research work to be framed within the potential unpredictability of interfacial failure. Moore and Williams [46] also provided insight about failure locations which prompted the belief that failure would occur at the

material interface for the majority of the specimens with constant TB+ volume. However, most tested fatigue specimens failed in the TB+ (flexible) region with an exception of only two fatigue specimens. Insufficient tested specimens and data failed to provide enough statistical significance to support a viable conclusion on the effect the use of FGMs has on the failure location in specimens.

In order to understand the trends in Figure 5-1 and Figure 5-2, failed fatigue specimens were observed under a digital microscope to gain insight into the behavior of the material gradients. Based on the observations, unpredicted elastomeric behavior was noted. Figure 5-3 and Figure 5-4 represent the specimens with continuous material gradients and specimens with discrete material gradients respectively.

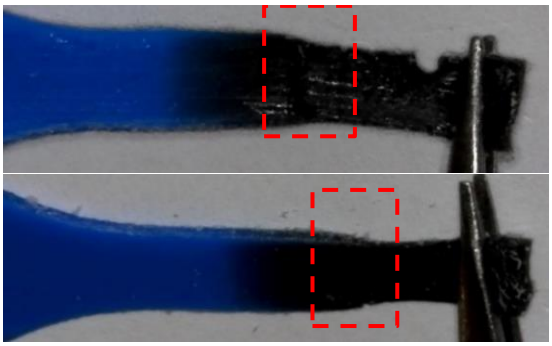

Figure **5-3**: Tested fatigue specimens with continuous material gradients showing failure in the flexible, TB+, region and a step discontinuity in the transition region.

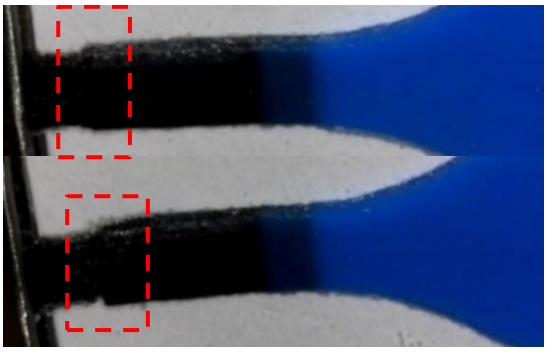

Figure **5-4**: Tested fatigue specimens with discrete material gradients showing failure in the flexible, TB+, region and a step discontinuity in the transition region.

It was assumed that when elongated during fatigue testing, the specimens would behave in an elastomeric manner in the flexible material region, especially where the TB+ material outnumbers the rigid material. However, contrary to the assumption, the qualitative observation of the failed specimens showed a visible step discontinuity in flexibility as the gradient material transition region approaches the flexible material region. During fatigue testing, the deformable flexible region reduced in length for both continuous and discrete material gradient specimens causing the step discontinuities. This indicated that there was no smooth transition in the designed material gradients and hence the material properties. It was also hypothesized that a linear change in the material distribution across the central region would result in a linear change in the material properties. The increase in the stress experienced in the flexible material region for both continuous and discrete material gradient specimens caused a decrease in the fatigue life. This qualitative observation is confirmed by the fatigue life data obtained for all tested specimens shown in Table 5-1 and represented in Figure 5-1and Figure 5-2.

Based on the data analysis and observations of the tested fatigue specimens with constant TB+ volume, specimens with a longer TB+ material length in the material gradient transition region, including the control specimens, withstood more cycles before failure thus a higher fatigue life compared to regions with a shorter TB+ material length. The reduction of flexible material in the central region led to the decrease in fatigue life caused by different gradient types and the material transition lengths. This conclusion led to another hypothesis that considered maintaining the length of the TB+ material alongside the continuous and discrete material gradients.

5.2 Data Analysis for Specimens with Constant TB+ Length

This section provides the data analysis and discussion of the results obtained from the fatigue testing procedure discussed in Section 4.2.2. This analysis helps determine the impact of different material gradient types on the fatigue life and interfacial behavior.

Table **5-3**: Data obtained for fatigue tested specimens with a constant TB+ length.

Material Gradient Types	*Lengths*	*No. of Specimens*	*Cycles to Failure*	*Failure Location*
Continuous Gradients	Max-length	Specimen – 1	914	TB+ Region
		Specimen – 2	1097	TB+ Region
		Specimen – 3	799	TB+ Region
		Specimen – 4	568	TB+ Region
		Specimen – 5	1029	TB+ Region
	Min-length	Specimen – 1	1155	TB+ Region
		Specimen – 2	594	TB+ Region
		Specimen – 3	221	TB+ Region
		Specimen – 4	1240	TB+ Region
		Specimen – 5	1675	TB+ Region
Discrete Gradients	Max-length	Specimen – 1	844	TB+ Region
		Specimen – 2	835	Interface
		Specimen – 3	524	Interface
		Specimen – 4	715	Interface
		Specimen – 5	1014	TB+ Region
	Min-length	Specimen – 1	1881	TB+ Region
		Specimen – 2	1023	TB+ Region
		Specimen – 3	1517	TB+ Region
		Specimen – 4	1096	TB+ Region
		Specimen – 5	1240	TB+ Region
Control Specimens		Specimen – 1	275	Interface
		Specimen – 2	1540	TB+ Region
		Specimen – 3	1306	TB+ Region
		Specimen – 4	1229	TB+ Region
		Specimen – 5	1294	Interface

Similar to the data analysis discussed in Section 5-3, two-way analysis of variance (ANOVA) was used to analyze statistical significance between the main interaction effects of different material gradient type and gradient lengths with respect to the number of cycles to failure. All of the assumptions made for using two-way ANOVA to analyze the data were met accordingly including the homogeneity of variance test, which was met since $p > 0.05$. The two-way ANOVA test showed no statistically significant difference

for all main interactions; the difference in maximum and minimum lengths had a p-value of 0.074 and the difference between the continuous and discrete gradients with a p-value of 0.435. Comparing both gradient types with the material transition lengths showed no statistical significance with a p-value of 0.196.

For this data set, four specimens had exceptionally lower cycles to failure; however, they were not omitted from the data analysis. This is because of a limited data set obtained and the fact that the two-way analysis of variance test requires equal numbers of groups for comparison. Similarly, the outlying data points with lower cycles to failure were likely caused by different aging effects and varying humidity levels compared to other specimens.

Table **5-4**: Statistics obtained from the fatigue testing procedure of specimens with a constant TB+ length.

		Fatigue life (# of cycles to failure)	
Material Gradient Types	*Lengths*	*Mean*	*Standard Deviation*
Continuous Gradients	Max-length	881.40	208.80
	Min-length	977	571.5
Discrete Gradients	Max-length	786.80	182.15
	Min-length	1069.10	351.21
Control Specimens		1128.80	491.6

Comparing results in Table 5-1 with results in Table 5-3, the number of samples of tested fatigue specimens was increased from 15 to 25 samples in order to expand on the results for better statistical analysis. With reference to the average number of cycles to failure, there is a noticeable increase in the fatigue life for the specimens with a constant

TB+ length. This is attributed to the increased length of TB+ material as opposed to the varying lengths of TB+ displayed in the specimens with a constant TB+ volume. The control specimens maintained an increased fatigue life; however, their fatigue performance was lower than the previous results obtained in Section 5.1. In addition, one of the specimens in the control group experienced premature interfacial failure. This might have been due to the different mechanical testing system used for fatigue testing of specimens with a constant length, which was accepted as an alternative testing system [17] but had a different loading rate.

Similarly, fatigue life was compared against all fatigue specimens groups with different volumes of TB+ in the material gradient transition region over a constant length of 100% TB+ as shown in Figure 5-5. The plot shows that maintaining the length of the flexible material improves the number of cycles to failure for all specimens groups; however, specimens with a minimum length of material gradient transitions still perform better than specimens with a maximum length of material gradient transitions, a similar observation in the results analyzed in Section 5-1.

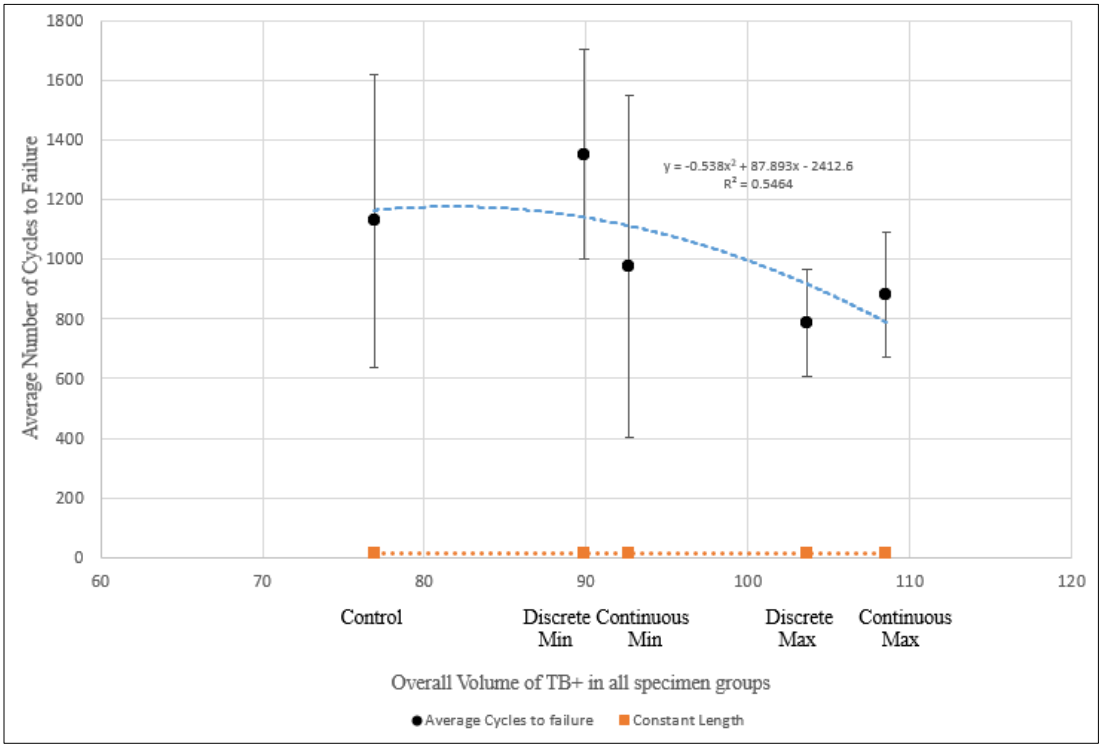

Figure **5-5**: The average number of cycles to failure with the standard deviations error bars based on the overall volume of TB+ in all fatigue specimens tested.

Furthermore, Figure 5-6 shows a plot comparing the average number of cycles for each specimen group. A similar observation is seen whereby specimens with a minimum length of gradient in the material transition region experienced a better fatigue life. From a design standpoint, specimens with a minimum length of material gradients had a longer region over which flexible material was distributed. On the other hand, specimens with a maximum or larger region of material transitions had a shorter region with flexible material. It has since been determined, as evidenced by the fatigue testing results, that a longer flexible region causes an increase in the fatigue life.

One other observation with the material gradient types, the continuous and discrete gradients, is that all specimens with discrete gradients had a larger average number of cycles to failure when compared against specimens with continuous gradients. This is mostly attributed to the design process and the selective combination of material percentages used to create the discrete gradient.

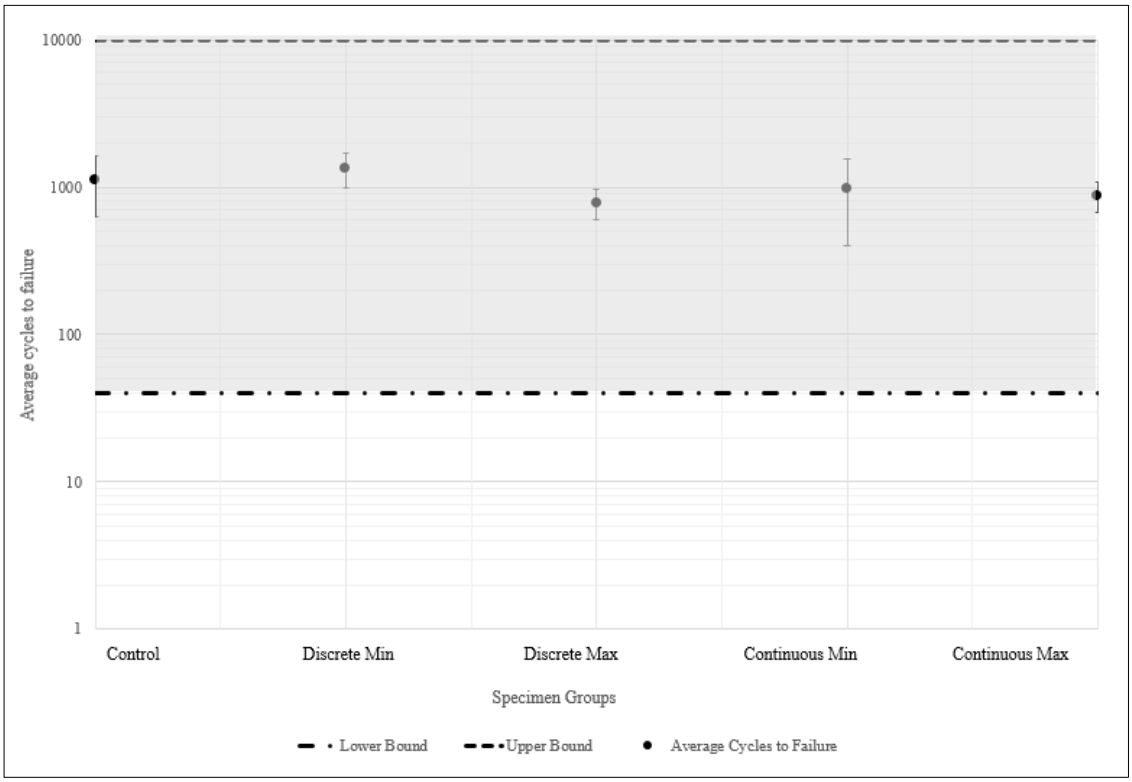

Figure **5-6**: The average cycles to failure with the standard deviations as error bars for all specimen tested.

The 95% confidence interval (CI) obtained from fatigue testing at 40% elongation by Moore and Williams [46] was also included in the plot, represented by the shaded grey region, to highlight any unpredictability of interfacial failure. In contrast with Figure 5-2, it is clear that the average number of cycles to failure for all specimen groups lie between

the upper and lower bounds of the 95% CI. None of the specimens with a constant TB+ volume experienced interfacial failure; however, within the category of specimens with a constant TB+ length, 30% of the specimens with discrete material gradients and 40% of the control specimens failed at the material interface.

Figure 5-7 is a supplementary graphical representation of all fatigue tested specimens with a constant volume or constant length of TB+ showing how the length of the region with 100% TB+, the overall volume of TB+ in the specimens, and the average number of cycles to failure relate in a three dimensional curve fitted surface.

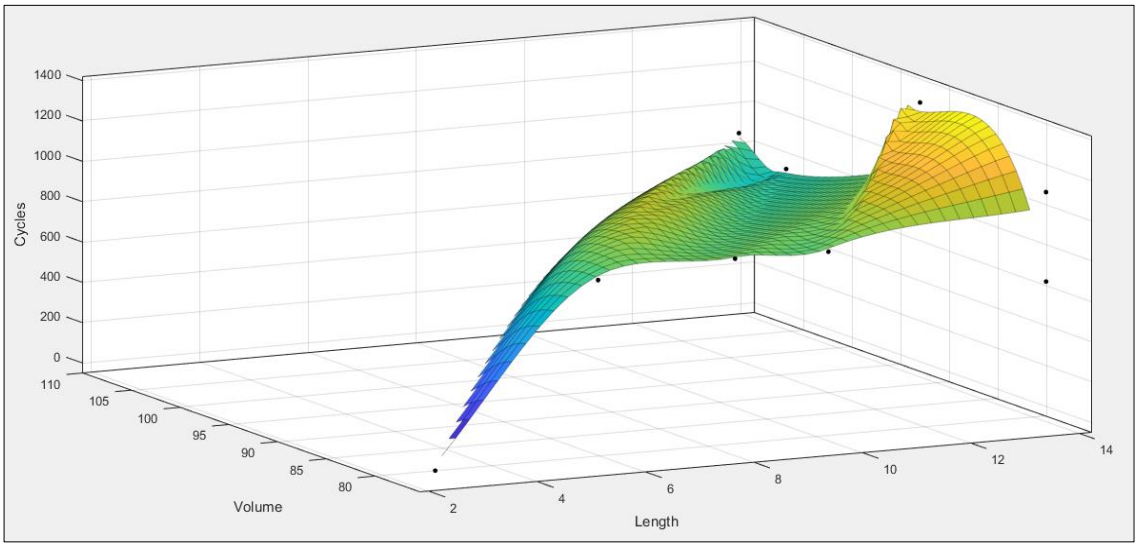

Figure **5-7**: Graphical representation of all fatigue tested specimens relating the length of the region with 100%TB+, the overall volume, and the average number of cycles to failure.

Interfacial failure was mostly attributed to the increase in the length of the flexible material in the central region, a design made such that in case of such failure, it could be

easily observed. Figure 5-8 shows examples of fatigue specimens that experienced interfacial failure

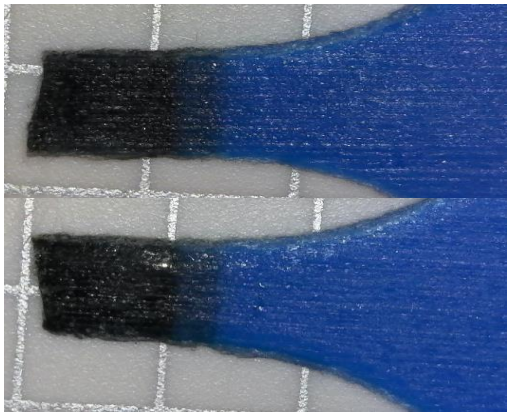

Figure **5-8**: Tested fatigue specimens showing failure at the material interface for discrete gradient specimens with a constant TB+ length.

In order to understand the trends in Figure 5-5 and Figure 5-6, the failure modes as well as the elastomeric behavior for all tested fatigue specimens were analyzed. By observing failed fatigue specimens, a similar step discontinuity was seen as the material gradients transition in the elastomeric region as seen in Figure 5-9 and Figure 5-10. This observation confirmed an uneven distribution in the material gradients as seen in the specimens with a constant TB+ volume as well as the material properties analyzed.

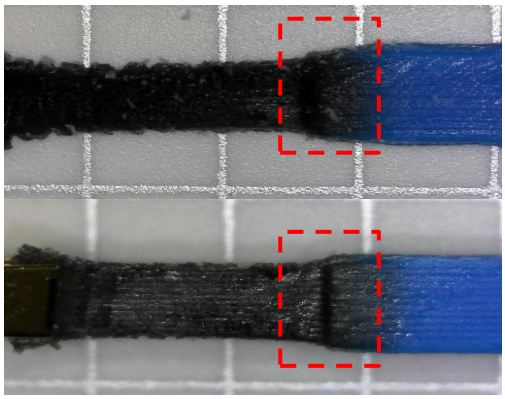

Figure **5-9**: Tested fatigue specimens with continuous material gradients showing a step discontinuity in the material gradient transition region.

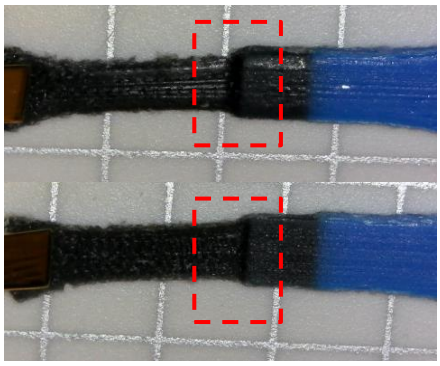

Figure **5-10**: Tested fatigue specimens with discrete material gradients showing a step discontinuity in the material gradient transition region.

Since the linear transition of the material compositions did not appear to equate to the linear change in the material properties, especially in the specimens with continuous and discrete material gradients, it was hypothesized that the material gradients in the transition region converge faster from the flexible to rigid material properties. This led to the analysis of individual material composites and their effect on the material properties.

5.3 Data Analysis for Specimens with Individual Material Composites

Based on the fatigue testing analysis of failed specimens with either constant TB+ volume or constant TB+ length, it was important to identify the relationship between the material compositions and the properties exhibited. To augment this, specimens with individual material composites were designed, fabricated, and their material properties analyzed. A tensile testing procedure was performed for such specimens as discussed in Section 4.3 and the results obtained are presented in Table 5-4. A total of 12 specimens were printed and tested with individual material compositions. Figure 5-11 shows examples of tensile tested specimens with different material composites.

Table **5-5**: Statistics obtained from the tensile testing procedure of specimens with individual material composites.

Material Composite Percentage	*Average Load (N)*	*Average Extension at Break (mm)*	*Average Maximum Tensile Stress (MPa)*
0.2	28.69	26.61	5.111
0.4	76.88	11.31	13.695
0.6	173.42	7.17	30.89
0.8	303.3	7.71	54.025

Figure **5-11**: Tensile tested specimens with different individual material composites.

Based on the results, the average maximum tensile stress was compared for each material composite. The plot shown in Figure 5-12 presents the comparison for specimens with material composites ranging from 20% to 80% of rigid material and features a quadratic trend line as the best fit curve and the accompanying equation.

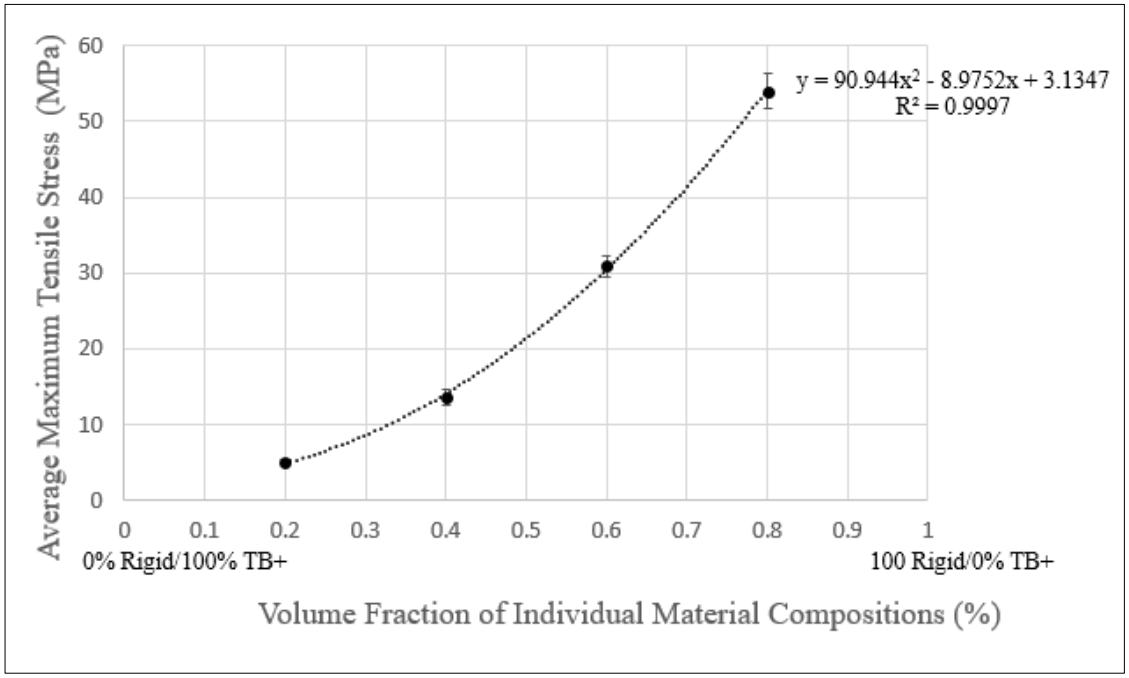

Figure **5-12**: The average maximum tensile stress for each individual material composite.

It is seen that as the material composite increases in rigidity, the maximum tensile stress experiences a quadratic increase. The behavior of the tested fatigue specimens is confirmed in that the material properties of linearly distributed material gradients are inherently not the same as the linear transitions of the actual gradients designed. The continuous and discrete material gradients were designed to follow linear patterns; however, this observation implies that the material gradients do not exhibit linear patterns in the material properties thereby not following the "Rule of Mixtures" [51].

The "Rule of Mixtures" phenomenon is an approach used to predict properties of composite materials. Based on the continuous and discrete material gradients designed, this approach was not used to predict the material properties of the specimens hence the differences seen. Figure 5-13 presents two gradient structures that show a difference in

the linear pattern based on the material composition and the actual material properties. The linear gradient pattern based on the material compositions (top) was employed in the design of specimens with both continuous and discrete material gradients. The linear gradient pattern (bottom) based on the material properties was generated from the analysis of the specimens with individual material composites.

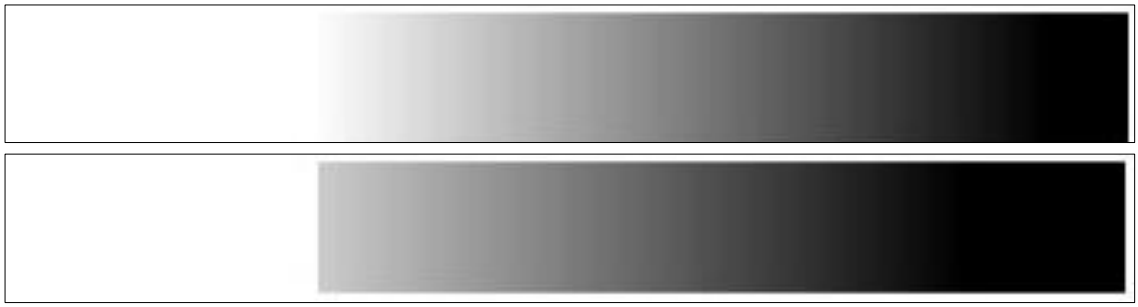

Figure **5-13**: Gradient based on material composition (top) and gradient based on actual material properties (bottom).

With reference to the linear gradient based on material properties (bottom image of Figure 5-12), a rapid jump from white to black is clearly seen. This implies that in order to achieve actual linear material properties, the flexible material should be incorporated sooner into the material transition region rather than later as was previously designed.

Chapter 6

CONCLUSIONS AND IMPLICATIONS

This research study aimed at relating the process, structure, property and behavior of multi-material parts by investigating the fatigue properties of functionally graded materials. Functional gradients of material compositions were designed from flexible and rigid materials, TangoBlackPlus (TB+) and VeroCyan (VC) respectively, and were fabricated using the Objet350 Connex3 PolyJet printer. The variation of the material properties depended on the selected percentage compositions of both material profiles. The flexible material, TB+, was distributed in the material gradient transition region of a specimen for two categories; (1) constant TB+ volume and (2) a constant TB+ length. The main focus was to investigate the fatigue life of specimens designed with either continuous or discrete material gradients dispersed across different lengths within the same material gradient transition region in the specimens. By investigating the material properties of selected material gradients, the behavior of the multi-material specimens would be determined.

The quantitative analysis of the specimens with a constant TB+ volume provided insight about the nature of multi-material specimens. More flexible material in the material gradient transition region led to an increase in the fatigue life; however, as the length of the material gradients increased the fatigue life decreased. The distribution of material gradients over a larger region with less flexible material, increased the stress experienced in the flexible material; hence, most specimens failed in the TB+ material

region. The failure location for any given material gradient in the transition region was unpredictable due to the different lengths over which the material gradients were distributed. Among this category, control specimens, which had the most distribution of the TB+ material with no gradient transition, experienced more flexibility and therefore had the most fatigue life compared to the specimens with continuous and discrete material gradients. Maintaining the volume of the flexible material in a linear pattern created a limitation in the distribution of material across a material gradient transition region since material properties for each material gradient did not smoothly transition from one to another.

The localized failure within the TB+ region was therefore dependent on the length of TB+ distributed in the central region of the specimens leading to the analysis of the specimens with a constant TB+ length. The goal, then, was to further investigate an improvement or decline in the fatigue life of multi-material specimens. It was observed that for each specimen group, the fatigue life was improved. This was mainly due to the increased length of TB+ material in the material gradient transition region. in addition to the material gradients distributed therein. Contrary to the results and findings, the analyses of specimens with a constant TB+ volume and a constant TB+ length showed a similar step discontinuity at the material interfaces where the flexible material, TB+ begins to outnumber the rigid material. In addition, micro cracks were observed at the interface, even though failure occurred in the TB+ material region. As discussed, it was expected that the linear material gradients would exhibit a smooth transition in the material properties.

The tensile tests performed on the specimens with individual material composites developed a correlation between the distribution of the material gradients and their actual material properties. A more even distribution of material properties was observed as the rigidity of the material composites increased. Initially, the material gradient transition region approached the rigid-like material properties faster than the linear transition, which caused the step discontinuity in the linear behavior of the material. This led to a conclusion that the material properties of linear distribution does not equal the linear distribution of the material gradient colors. However, by adding flexible material earlier in the material gradient transition region, the right set of material properties are produced.

The conclusions obtained from the findings and observations in this research work have led to a better understanding of tailoring different material gradient types in such a way that failure occurs in certain locations and the fatigue life is maximized. With reference to the living hinge designs with an improved fatigue life, it is important to consider increasing flexibility at the living hinge since the introduction of rigid material weakens the region in which a material composite is added. The overall design process of multi-material parts with both flexible and rigid FGMs involves the critical analysis of the intended material properties as well as the expected performance of the FGM parts. By doing so, specific material composites can be selected to ensure that the as-manufactured part matches the as-designed geometry. For better results in terms of improved fatigue life, having a region with a larger and consistent flexible material with

a minimum amount of material gradients is the best procedure to consider when designing multi-material parts.

With these conclusions in mind, engineers and designers could potentially focus on tailoring the material gradient types such that fatigue life is maximized and the material properties are as expected. In order to expand the breadth of this research, additional experimentation in terms of fatigue tests could be conducted to study the effects of different strain levels on the fatigue life. Similarly, additional experimentation of multi-material specimens are required to analyze the fatigue life at different strain levels. Better design methodologies for different material gradient types are necessary to further improve the quality of manufactured multi-material parts based on the desired material properties. Furthermore, the characterization of the materials is important to consider in order to understand the general process of measuring different structures and properties of materials. Lastly, studying voxel-based manufacturing of functionally graded structures is important to compare designed geometries with the manufactured parts.

REFERENCES

[1] Gibson, I., Rosen, D. W., and Stucker, B., 2010, "Additive Manufacturing Technologies," Additive Manufacturing Technologies: Rapid Prototyping to Direct Digital Manufacturing, pp. 1–459.

[2] Doubrovski, E. L., Tsai, E. Y., Dikovsky, D., Geraedts, J. M. P., Herr, H., and Oxman, N., 2015, "Voxel-Based Fabrication through Material Property Mapping: A Design Method for Bitmap Printing," CAD Computer Aided Design.

[3] Park, S.-I., and Rosen, D. W., 2015, "Quantifying Mechanical Property Degradation of Cellular Material Using as-Fabricated Voxel Modeling for the Material Extrusion Process," Annual solid freeform fabrication symposium, pp. 1070–1091.

[4] Gao, H., Kaweesa, D. V, Moore, J., and Meisel, N. A., 2016, "Investigating the Impact of Acetone Vapor Smoothing on the Strength and Elongation of Printed ABS Parts," JOM: The Journal of the Minerals, Metals & Materials Society, **69**(3), pp. 580–585.

[5] International, A., 2013, "Standard Terminology for Additive Manufacturing Technologies - ASTM F2792-12a," pp. 2–4.

[6] Barclift, M. W., and Williams, C. B., 2012, "Examining Variability in the Mechanical Properties of Parts Manufactured via PolyJet Direct 3D Printing."

[7] Meisel, N. A., and Williams, C. B., 2015, "Design for Additive Manufacturing: An Investigation of Key Manufacturing Considerations in Multi-Material Polyjet 3D Printing," Proceedings of the International Solid Freeform Fabrication Symposium, **26**, pp. 746–763.

[8] Blanco, D., Fernandez, P., and Noriega, A., 2014, "Nonisotropic Experimental Characterization of the Relaxation Modulus for PolyJet Manufactured Parts," Journal of Materials Research, **29**(17), pp. 1876–1882.

[9] Stratasys, "PolyJet Technology."

[10] Miyamoto, Y;Kaysser, W.A;Rabin, B.H;Kawasaki, A;Ford, R. ., 1996, *Functionally Graded Materials: Design, Processing, and Applications*, Kluwer Academic, Osaka.

[11] Jha, D. K., Kant, T., and Singh, R. K., 2013, "A Critical Review of Recent Research on Functionally Graded Plates," Composite Structures, **96**, pp. 833–849.

[12] Kumar Bohidar, S., Sharma, R., and Mishra, P. R., 2014, "Functionally Graded Materials: A Critical Review," International Journal of Scientific Footprints, **2**(4), pp. 18–29.

[13] Birman, V., "Functionally Graded Materials and Structures," Encyclopedia of Thermal Stresses, pp. 1858–1865.

[14] Birman, V., and Byrd, L. W., 2007, "Modeling and Analysis of Functionally

Graded Materials and Structures," Applied Mechanics Reviews, **60**(5), pp. 195–215.

[15] Gibson, I., Goenka, G., Narasimhan, R., and Bhat, N., 2010, "Design Rules for Additive Manufacture," 21st Annual International Solid Free Form Fabrication Symposium, Austin, TX, pp. 705–716.

[16] Lobontiu, N., 2002, *Compliant Mechanisms: Design of Flexure Hinges*, CRC Press LLC.

[17] ASTM International, 2011, "ASTM D4482-11 Test Method for Rubber Property — Extension Cycling Fatigue," Annual Book of ASTM Standards, pp. 1–10.

[18] Mahamood, R. M., and Akinlabi, E. T., 2017, *Functionally Graded Materials*, Springer International Publishing AG.

[19] Vel, S. S., and Goupee, A. J., 2008, "Multiscale Design of Functionally Graded Materials," Proceedings of 2008 NSF Engineering Research and Innovation Conference, Knoxville, Tennessee, pp. 3–6.

[20] Watanabe, Y., Inaguma, oshifumi, Sato, H., and Miura-Fujiwara, E., 2009, "A Novel Fabrication Method for Functionally Graded Materials under Centrifugal Force: The Centrifugal Mixed-Powder Method," Materials, **2**(4), pp. 2510–2525.

[21] Miyamoto, Y., 1996, *Functionally Graded Materials*.

[22] Mahamood, R. M., Member, E. T. A., Shukla, M., and Pityana, S., 2012, "Functionally Graded Material : An Overview," World Congress on Engineering, **III**, pp. 2–6.

[23] Markworth, A. J., Ramesh, K. S., and Parks, W. P., 1995, "Modelling Studies Applied to Functionally Graded Materials," Journal of Materials Science, **30**(9), pp. 2183–2193.

[24] Kawasaki, A., and Watanabe, R., 1987, "Finite Element Analysis Of Thermal Stress Of The Metal/Ceramic Multi-Layer Composites With Controlled Compositional Gradients," Nippon Kinzoku Gakkai-si.

[25] Tanaka, K., Tanaka, Y., Watanabe, H., Poterasu, V. F., and Sugano, Y., 1993, "An Improved Solution to Thermoelastic Material Design in Functionally Gradient Materials: Scheme to Reduce Thermal Stresses," Computer Methods in Applied Mechanics and Engineering, **109**(3–4), pp. 377–389.

[26] Maciejewski, G., 2012, "Optimization of Functionally Gradient Materials under Cyclic Thermal and Mechanical Loading," (September), pp. 421–430.

[27] Pratap, A., 2003, "Implementation of a Functionally Gradient Material Modeling and Design System," Mechanical Engineering.

[28] Huang, J., Fadel, G. M., Blouin, V. Y., and Grujicic, M., 2002, "Bi-Objective Optimization Design of Functionally Gradient Materials," Materials and Design, **23**(7), pp. 657–666.

[29] Hirano, T., and Yamada, T., 1988, "Multi Paradigm Expert System Architecture

Based Upon The Inverse Design Concept," Artificial Intelligence for Industrial Applications, 1988. IEEE AI'88., Proceedings of the International Workshop on, pp. 245–250.

[30] Tanaka, K., Tanaka, Y., Enomoto, K., Poterasu, V. F., and Sugano, Y., 1993, "Design Of Thermoelastic Materials Using Direct Sensitivity And Optimization Methods. Reduction Of Thermal Stresses In Functionally Gradient Materials," Computer Methods in Applied Mechanics and Engineering, **106**(1–2), pp. 271–284.

[31] Kieback, B., Neubrand, A., and Riedel, H., 2003, "Processing Techniques For Functionally Graded Materials," Materials Science and Engineering, **362**(1–2), pp. 81–105.

[32] Mahamood, Rasheedat M; Akinlabi, E. T., 2012, "Functionally Graded Material: An Overview," Proceedings of the World Congress on Engineering, **3**.

[33] Garland, A., and Fadel, G., 2015, "Manufacturing Functionally Gradient Material Objects with an off the Shelf 3D Printer: Challenges and Solutions," *ASME 2015 International Design Engineering Technical Conferences & Computers and Information in Engineering Conference*, Boston, pp. 1–10.

[34] Vaezi, M., Chianrabutra, S., Mellor, B., and Yang, S., 2013, "Multiple Material Additive Manufacturing – Part 1: A Review," Virtual and Physical Prototyping, **8**(1), pp. 19–50.

[35] Shin, K. H., Natu, H., Dutta, D., and Mazumder, J., 2003, "A Method for the Design and Fabrication of Heterogeneous Objects," Materials and Design, **24**, pp. 339–353.

[36] Bruyas, A., Francois, G., and Renaud, P., 2014, "Towards Statically Balanced Compliant Joints Using Multimaterial 3D Printing," *ASME 2014 International Design Engineering Technical Conferences & Computers and Information in Engineering Conference*, pp. 1–10.

[37] Kawasaki, A., and Watanabe, R., 1997, "Concept and P/M Fabrication of Functionally Gradient Materials," Ceramics International, **23**(1), pp. 73–83.

[38] Gay, P., Blanco, D., Pelayo, F., Noriega, A., and Fernandez, P., 2015, "Analysis of Factors Influencing the Mechanical Properties of Flat PolyJet Manufactured Parts," Procedia Engineering, **132**, pp. 70–77.

[39] Kesy, A., and Kotlinski, J., 2010, "Mechanical Properties of Parts Produced by Using Polymer Jetting Technology," Archives of Civil and Mechanical Engineering, **10**(3), pp. 37–50.

[40] Bass, L. B., Meisel, N. A., and Williams, C. B., 2015, "Exploring Variability in Material Properties of Multi-Material Jetting Parts," Solid Freeform Fabrication Symposium, **1**(Figure 1), pp. 993–1006.

[41] Pilipović, A., Raos, P., and Šercer, M., 2009, "Experimental Analysis of Properties of Materials for Rapid Prototyping," The International Journal of Advanced Manufacturing Technology, **40**(1–2), pp. 105–115.

[42] Gent, A. N., Lindley, P. B., and Thomas, A. G., 1964, "Cut Growth and Fatigue of Rubbers. I. The Relationship Between Cut Growth and Fatigue," Journal of Applied Polymer Science, **8**(1), pp. 455–466.

[43] Wang, F., 2012, "Mechanical Property Study on Rapid Additive Layer Manufacture Hastelloy(R) X Alloy by Selective Laser Melting Technology," International Journal of Advanced Manufacturing Technology, **58**(5–8), pp. 545–551.

[44] Santos, E., Abe, F., Kitamura, Y., Osakada, K., and Shiomi, M., 2002, "Mechanical Properties of Pure Titanium Models Processed by Selective Laser Melting," Proceedings of the Annual International Solid Freeform Frabrication Symposium, pp. 180–186.

[45] Moore, J. P., and Williams, C. B., 2008, "Fatigue Characterization of 3D Printed Elastomer Material," Proceedings of the Annual International Solid Freeform Frabrication Symposium, pp. 641–655.

[46] Moore, J. P., and Williams, C. B., 2015, "Fatigue Properties of Parts Printed by PolyJet Material Jetting," Rapid Prototyping Journal, **3**, pp. 1–16.

[47] Callister, W. D., and Rethwisch, D., 2007, *Materials Science and Engineering: An Introduction*, John Wiley & Sons Inc.

[48] ASTM D4482-11, 2011, "Standard Test Method for Rubber Property — Extension Cycling Fatigue," Annual Book of ASTM Standards, **i**(C), pp. 1–9.

[49] Floyd, R.W; Steinberg, L., 1976, "An Adaptive Algorithm for Spatial Grayscale," Proceedings of the Society for Information Display, **17**, pp. 75–77.

[50] ASTM D638, 2004, "Standard Test Method for Tensile Properties of Plastics," Annual Book of ASTM Standards, pp. 1–15.

[51] Kim, H. S., Hong, S. I., and Kim, S. J., 2001, "On the Rule of Mixtures for Predicting the Mechanical Properties of Composites with Homogeneously Distributed Soft and Hard Particles," Journal of Materials Processing Technology, **112**(1), pp. 109–113.

This research was conducted on the Stratasys Objet350 Connex3 printer through Stratasys' Voxel Print Research Program, which enhances the value of 3D printing as a powerful platform for experimentation, discovery, and innovation. For more information, contact Stratasys Education Academic Research and Development Unit: academic.research@stratasys.com. Any opinions, findings, and conclusions or recommendations expressed in this material are those of the author and do not necessarily reflect the views Stratasys.